中國醫藥大學營養學系碩士班

碩 士 論 文

薑黃素和鼠尾草酸抑制細胞激素誘發之人類大主動脈平滑肌細胞的遷移和基質金屬蛋白酶的活化

Curcumin and Carnosic acid inhibit MMP-9 activity and migration of cytokine-induced human aortic smooth muscle cells

研究生：林杏純
(Hsing-Chun, Lin)

指導教授：余雅美　博士
(Ya-Mei, Yu)

中 華 民 國　　96　年　06　月　22　日

謝　誌

感謝指導教授余雅美博士兩年來於學業、研究等方面的悉心指導及待人處事上的諄諄教誨，使本論文得以順利完成。師恩浩瀚，永銘於心，謹誌卷首，以表誠摯之謝忱。

文稿初成，承蒙台灣大學沈立言教授與中國醫藥大學江素瑛助理教授於百忙之中撥冗審閱，詳加斧正，並提供寶貴意見使論文內容得以更加完善，謹此致上萬分謝意。

在學期間，多蒙學長姐的指導與同窗好友芩卉、珮玲、馨儀、美瑜、美存、珊瑩、昇輝及同期研究所同學於實驗與生活上的幫助與支持；實驗室之學妹瑜妏、于婷、郁婷、珮琪、榆茜的協助與幫忙；再者，要感謝好友們佩文、映廷、子綺、Yurika、怡真、美玲，於艱辛研究過程中給予諸多的協助與鼓勵，在此致上最誠摯的謝意。

最後由衷感謝男友育成及其家人伯父、伯母及俊宏，還有我最親愛的家人們村村爸、珍珍媽、阿憲弟弟以及綉妃的關懷與支持，使我能安心無慮的完成學業。謹此將本論文獻給所有關心及曾經幫助我的人，謝謝你們。

<div style="text-align: right">

林杏純　謹致於
中國醫藥大學 營養學系
中華民國 九十六年六月

</div>

Contents

Table of contents

Figure of contents

Appendix

摘要

　　動脈粥狀硬化在美國及其他西方國家中是造成死亡的主要疾病。血管平滑肌細胞的遷移和基質金屬蛋白酶的活化，在動脈粥狀硬化的發展中扮演一個重要的角色。薑黃素是衍生自薑黃的多酚，目前已有數百萬人會每天攝取。一般而言，薑黃素與數種生物和細胞活性有關，包含抗氧化、抗發炎、抗癌，以及降低血中膽固醇的特性。鼠尾草酸是存在鼠尾草與迷迭香中的主要酚類化合物，在過去的體外試驗中已被證實具抗氧化的能力。本研究之目的主要探討薑黃素和鼠尾草酸抑制 TNF-α 誘發人類大主動脈的平滑肌細胞的遷移與基質金屬蛋白酶-9 (MMP-9) 的相關性。在遷移試驗中顯示薑黃素和鼠尾草酸可有效抑制 TNF-α 誘發之平滑肌細胞的遷移。由 Gelatin zymography 試驗顯示薑黃素和鼠尾草酸會降低 MMP-9 的分泌，且西方墨點法也顯示薑黃素和鼠尾草酸會降低 MMP-9 的表現。經 NF-κB 酵素免疫分析試驗證實，薑黃素和鼠尾草酸能減少核轉錄因子 NF-κB p50 與 p65 的活化，以及活性氧物種的產生。總而言之，薑黃素和鼠尾草酸降低平滑肌細胞的遷移是經由抑制 TNF-α 誘發 p50 和 p65 的核轉位，而抑制 MMP-9 的分泌及蛋白質表現。因此，薑黃素和鼠尾草酸在預防動脈粥狀硬化中，具有抗發炎的特性且可能扮演一個重要的角色。

關鍵字：動脈粥狀硬化、平滑肌細胞遷移、基質金屬蛋白酶、薑黃素、鼠尾草酸、核轉錄因子-κB、活性氧成分、腫瘤壞死因子-α。

Abstract

In the United States and other Western countries, atherosclerosis is the leading cause of illness and death. The migration and matrix metalloproteinases (MMPs) activation of vascular smooth muscle cells (VSMCs) may play key roles in the development of atherosclerosis. Curcumin, which is consumed daily by millions of people, is a polyphenol derived from the plant *Curcuma longa*. In general, curcumin has been associated with a large number of biological and cellular activities, including antioxidative, anti-inflammatory, anticarcinogenic, and hypocholesterolemic properties. Carnosic acid (CA) is the primary phenolic compound in rosemary and salvia. Previous study indicated that CA possesses antioxidant activity *in vitro*. In this study, we investigated the inhibitory effect of curcumin and CA on tumor necrosis factor-α (TNF-α)-induced the migration in human aortic smooth muscle cells (HASMCs) and MMP-9 activity. The migration assay showed that curcumin and CA effectively inhibited the TNF-α-induced migration of HASMCs as compared with the control group. Curcumin and CA lowered the secretion and protein expression of MMP-9 by gelatin zymography and western blot assays. They also decreased nuclear translocation of nuclear factor-κB (NF-κB) p50, p65, and ROS production. In conclusion, curcumin and CA inhibit TNF-α-induced nuclear translocation of p50 and p65, thereby suppressing the secretion and protein expression of MMP-9, resulting in decreased HASMCs migration. Thus, curcumin and CA have anti-inflammatory properties and may play important roles in the prevention of atherosclerosis.

Chapter 1

Literature review

1.1 Morphology of artery

The structure of the normal blood wall comprises three layers: the innermost layer is called the intima, the middle layer is called the media, and the outermost layer is known the adventitia (Fig. 1). The intima is an inner monolayer of endothelial cells lining the lumen and is bound on the outside by internal elastic lamina, a fenestrated sheet of elastin fibers. The thin subendothelial space in between contains thin elastin and collagen fibers along with a few smooth muscle cells (SMCs). The extracellular matrix (ECM) of the vascular wall, largely elastin and collagen, subserves many functions essential for vessel homeostasis. ECM damage or remodeling in conditions such as rheumatoid arthritis (Weber and De Bandt, 2000), malignant tumors (Ohtani, 1998), aortic aneurysm (MacSweenety, 1994), and atherosclerosis (Libby, 1995; 2000) contributes to the formation, progression, and clinical expressions of these disorders.

1.2 Oxidative stress and atherosclerosis

Several lines of evidence indicate that oxidative stress may play an important role in various pathological conditions, including cancer, neurodegeneration, atherosclerosis, diabetes, rheumatoid arthritis, postischemic reoxygenation injury, and aging. Oxidative stress may lead to many cellular events, such as inactivation of NO,

oxidative modifications of DNA and proteins, lipid oxidation, enhanced mitogenicity and apoptosis of vascular cells, and increased expression and activation of redox-sensitive genes, such as the receptor for oxidized LDL, adhesion molecules, chemotaxis factors, NF-κB (Muller *et al*, 1997), proinflammatory cytokines, regulators of cell cycle progression, and matrix metalloproteinases (Wassmann *et al*, 2004).

Vascular lesions form during pathological processes, which involve the accumulation of inflammatory cells and release of cytokines. Production of cytokines and growth factors within lesions may induce migration of SMCs. Proinflammatory cytokines, such as tumor necrosis factor (TNF) and interleukin-1 (IL-1), play important roles in the pathogenesis of atherosclerosis (Zhu *et al*, 1999; Rahman *at al*, 1998). TNF-α, an inflammatory cytokine released in greater quantities by obese humans and patients with insulin resistance, not only initiates but also propagates atherosclerotic lesion formation (Lau *et al*, 2005).

Cardiovascular disease (CVD) due to atherosclerosis is the leading cause of death in the Western world and the second most common cause worldwide (Braunwald, 1997). Atherosclerosis comes from the Greek words athero (meaning gruel or paste) and sclerosis (hardness). Almost 200 years ago, London surgeon J. Hodgson observed the inflammatory characteristics of atherosclerotic lesions (Kaperonis *et al*, 2006). A causative role of inflammation and infection in the pathogenesis of atherosclerosis was first proposed in 1908 by Sir William Osler (Kaperonis *et al*, 2006). Atherosclerosis is a chronic inflammatory disease driven by risk factors that cause oxidative and inflammatory mechanisms. The major risk factors are gender, age (Lusis *et al*, 2004), obesity (Yudkin *et al*, 1999), cigarette smoking (Nordskog *et al*, 2003), exercise, hypercholesterolemia (Khoo *et al*, 1988) ,

hypertension (Griendling *et al*, 1997), hyperglycemia (Schmidt *et al*, 1999), hyperhomocysteinemia (Majors *et al*, 1997), and bacterial and viral infection (Jackson *et al*, 1997). The pathobiology of atherosclerosis comprises endothelial cells dysfunction, SMCs proliferation and migration, fibrous cap formation, plaque rupture and thrombosis.

SMCs are important actors in the pathogenesis of atherosclerosis and restenosis after angioplasty or stent application (Hao *et al*, 2003). SMCs can synthesize and secrete biologically active mediators that regulate contraction and relaxation, inflammation, proliferation, apoptosis and matrix alterations (Dzau *et al*, 2002) (Fig. 2). The migration of SMCs from the tunica media to the subendothelial region is a key event in the development and progression of many vascular diseases including atherosclerosis and post-angioplasty restenosis (Maeda *et al*, 2002).

1.3 Matrix metalloproteinases (MMPs) and atherosclerosis

MMPs were discovered in 1962, in an effort to establish how the metamorphosing tadpole of a frog lost its tail (Jones *et al*, 2003). MMPs are a family of Zn^{2+}-dependent endopeptidases capable of cleaving components of ECM (Falk, 1999; Creemers *et al*, 2001). MMPs activity is regulated at three levels: gene transcription, activation of the latent proenzymes, and inhibition of proteolytic activity (Dollery *et al,* 1995; Birkedal-Hansen *et al*, 1993) (Fig. 3). MMPs can be categorized into the following groups: interstitial collagenases, gelatinases, stromelysins, membrane-type matrix metalloproteinases (MT-MMPs), and others. The collagenases include MMP-1, MMP-8, and MMP-13. Gelatinases are composed of MMP-2 and

MMP-9. The stromelysin group is composed of MMP-3, MMP-10, and MMP-11. Six different membrane type (MT)-MMPs are MT-MMP1, MT-MMP2, MT-MMP3, MT-MMP4, MT-MMP5, and MT-MMP6. And others are MMP-7, MMP-12, MMP-19, MMP-20, MMP-23, and MMP-26 (Creemers *et al*, 2001) (Table 1).

On the other hand, the activity of MMPs is controlled by specific inhibitors known as tissue inhibitors of MMPs (TIMPs). Three members of TIMPs have been identified to date: TIMP-1, TIMP-2, and TIMP-3. The balance between production of MMPs and TIMPs represents a critical point to maintain the homeostasis of the ECM (Birkedal-Hansen *et al*, 1993).

MMPs activity may contribute to the pathogenesis of atherosclerosis by facilitating migration of VSMCs (Jones *et al*, 2003). MMPs (MMP-9 and MMP-2) production and SMCs migration may play key roles in the pathogenesis of neointima formation and atherosclerosis. Especially inducible MMP-9 expression was directly involved in the cancer cell invasion and SMCs migration through vascular wall (Cho and Reidy, 2002; Galis *et al*, 2002). Although MMP-2 and MMP-9 have similar substrate specificities, there are differences in the regulation of their expression. MMP-2 is constitutively expressed by several cell types, including SMCs, and its expression is not induced by cytokines or growth factors. In contrast, based on reports from several different laboratories, it has generally been concluded that the basal levels of MMP-9 are usually low, and its expression can be induced by treatment of cells with TNF-α, but not platelet-derived growth factor (PDGF) or thrombin (Cho *et al*, 2000; Galis *et al*, 1994).

1.4 Nuclear factor-κB (NF-κB) and inflammation

Nuclear factor-κB (NF-κB) was first described in 1986 as a nuclear factor necessary for immunoglobulin kappa light chain transcription in B cells (hence the name, NF-κB) (Ghosh *et al*, 1998). Transcription factors are proteins responsible for the coordinated expression of genes through specific binding to gene promoter and enhancer sites. Transcription factor NF-κB and its target genes are involved in the pathogenesis of atherosclerosis (Kutuk and Basaga, 2003). The NF-κB family members include RelA (p65), RelB, c-Rel, p50 (NF-κB1), and p52 (NF-κB2), the latter two being synthesized from the inactive precursor molecules P105 and P100, respectively, as well as their inhibitory subunits IκBα, IκBβ, and IκBε (Martin *et al*, 2000). Each family member contains an N-terminal 300 amino acid conserved region known as the rel homology domain (RHD) (Ghosh *et al*, 1998). NF-κB subunits form homo- and heterodimers, the most prominent one is p50/p65 heterodimers (Fig. 4). The dimmer is retained in the cytoplasm in an inactive state through interaction with IκB. NF-κB is rapidly activated in response to variety of inflammatory and other stimuli that lead to degradation of IκB (Martin *et al.*, 2000). Active DNA-binding complexes of the NF-κB/Rel family consist of different homo- and heterodimers that bind to a common κB site (5'-GGGPuNNPyPyCC-3'), where Pu is purine, Py is pyrimidine and N is any nucleotide (Ghosh *et al.*, 1998). The nuclear translocation of NF-κB is induced by many agents, including inflammatory cytokines (*e.g.* TNF-α and IL-1), mitogens, bacterial products, protein synthesis inhibitors, oxidative stress (H_2O_2), ultraviolet light, and phorbol esters (Baeuerle, 1991; Grilli *et al*, 1993). Upon activation of NF-κB, a large number of genes are induced including various

inflammatory cytokines, adhesion molecules, and MMPs (Baeuerle, 1991; Grilli *et al*, 1993; Martin *et al*, 2000). The NF-κB is known regulator of inflammation, which represent key features of the response to vascular complications.

1.5 Curcumin

The characteristic yellow color of turmeric is due to the curcuminoids, first isolated by Vogel in 1842. Curcumin is an orange-yellow crystalline powder practically insoluble in water. The structure of curcumin ($C_{21}H_{20}O_6$) (Fig. 5) was first described in 1910 by Lampe and Milobedeska and shown to be diferuloylmethane (Aggarwal *et al*, 2003). Curcumin (diferuloylmethane) is the active yellow pigment in turmeric (the ground rhizome of *Curcuma longa* Linn), a popular plant-derived coloring spice and ingredient of many cosmetics and pharmaceuticals (Gafner *et al*, 2004; Shishodia *et al*, 2005; Aharma *et al*, 2005; Aggarwal and Shishodia, 2006; Maheshwari *et al*, 2006). Previous study also indicated that supplementation with *Curcuma longa* reduced oxidative stress and attenuates the development of fatty streaks in rabbits fed a high cholesterol diet (Quiles *et al*, 2002). In general, curcumin has been associated with a large number of biological and cellular activities, including antioxidative, anti-inflammatory, anticarcinogenic, and hypocholesterolemic properties (Gafner *et al*, 2004; Shishodia *et al*, 2005; Aharma *et al*, 2005; Aggarwal and Shishodia, 2006; Maheshwari *et al*, 2006). Curcumin mediates its effects by modulating several important molecular targets, including transcription factors, enzymes, cell cycle proteins, cytokines, receptors, and cell surface adhesion molecules (Shishodia *et al*, 2005; Aharma *et al*, 2005; Aggarwal and Shishodia, 2006).

1.6 Carnosic acid (CA)

Sage (*Salvia officinalis* L.) and rosemary (*Rosmarinus officinalis* L.) are popular Labiatae herbs used as spices and folk medicines around the world (Masuda *et al*, 2002). In the 1950s, it was reported that an extract of rosemary leaves contained high antioxidant activity (Huang *et al*, 2005). Extracts of Labiatae herbs can have both flavoring and antioxidant properties, and there has been particular interest in the use of rosemary extract over recent years. CA (Fig. 6) is a phenolic diterpene compound present in rosemary and sage leaves. CA has a typical *O*-diphenol structure and most diphenol compounds show potent chain-breaking antioxidant activity in food systems (Shahidi *et al*, 1992). This molecule has antimicrobial activity (Oluwatuyi *et al*, 2004; Moreno *et al*, 2006), is able to inhibit lipid absorption in humans (Ninomiya *et al*, 2004) and is a free radical scavenger, due to its phenolic skeleton (Masuda *et al*, 2001, 2002; del Bano *et al*, 2003). CA is a lipophilic antioxidant that scavenges singlet oxygen, hydroxyl radicals, and lipid peroxyl radicals, thus preventing lipid peroxidation and disruption of biological membranes (Aruoma *et al*, 1992; Haraguchi *et al*, 1995). Its radical scavenging activity follows a mechanism analogous to that of other antioxidants such as α-tocopherol and is caused by the presence of two *O*-phenolic hydroxyl groups found at C_{11} and C_{12} of the molecule (Richheimer *et al*, 1999).

1.7 The objective of this research

Atherosclerosis, a progressive pathological disorder leading to cardiovascular

and cerebrovascular diseases, is still the leading cause of mortality and morbidity in industrialized countries, in spite of improved pharmacological and lifestyle approaches (Ross, 1993). It is a chronic inflammatory disease driven by risk factors that cause oxidative and inflammatory mechanisms. Oxidative stress may lead to many cellular events, such as inactivation of NO, oxidative modifications of DNA and proteins, lipid oxidation, enhanced mitogenicity and apoptosis of vascular cells, and increased expression and activation of redox-sensitive genes, such as the receptor for oxidized LDL, adhesion molecules, chemotaxis factors, proinflammatory cytokines, regulators of cell cycle progression, and matrix metalloproteinases (Wassmann *et al*, 2004). Previous studies also indicated that proinflammatory cytokines, such as tumor necrosis factor (TNF) and interleukin-1 (IL-1), play an important role in the pathogenesis of atherosclerosis (Zhu *et al*, 1999; Rahman *at al,* 1998).

The migration of SMCs from the tunica media to the subendothelial region is a key event in the development and progression of many vascular diseases including atherosclerosis and post-angioplasty restenosis (Maeda *et al*, 2002). MMPs activity may contribute to the pathogenesis of atherosclerosis by facilitating migration of vascular smooth muscle cells (VSMCs) (Jones *et al*, 2003). MMPs (MMP-9 and MMP-2) production and SMCs migration may play key roles in the pathogenesis of neointima formation and atherosclerosis. The activity of the 92 kDa (MMP-9) but not the 72 kDa (MMP-2) gelatinase is induced by IL-1α, TNF-α and phorbol esters, in a variety of cell types (Birkedal-Hansen *et al*, 1993; Fabunmi *et al*, 1996).

Transcription factor NF-κB and its target genes are involved in the pathogenesis of atherosclerosis (Kutuk and Basaga, 2003). NF-κB subunits form homo- and heterodimers, the most prominent one is p50/p65 heterodimers. The dimmer is

retained in the cytoplasm in an inactive state through interaction with IκB. NF-κB is rapidly activated in response to a variety of inflammatory and other stimuli that lead to degradation of IκB (Martin *et al*, 2000). Upon activation of NF-κB, a large number of genes are induced including various inflammatory cytokines, adhesion molecules, and MMPs (Baeuerle, 1991; Grilli *et al*, 1993; Martin *et al*, 2000).

Curcumin, which is consumed daily by millions of people, is a polyphenol derived from the plant *Curcuma longa*. In general, curcumin has been associated with a large number of biological and cellular activities, including antioxidative, anti-inflammatory, anticarcinogenic, and hypocholesterolemic properties (Gafner *et al*, 2004; Shishodia *et al*, 2005; Aharma *et al*, 2005; Aggarwal and Shishodia, 2006; Maheshwari *et al*, 2006). In this study, we investigated the inhibitory effect of curcumin on TNF-α-induced human aortic smooth muscle cells (HASMCs) migration and MMP-9 activity.

Carnosic acid (CA) is the primary phenolic compound in rosemary and salvia. Previous study indicated that CA has a typical *O*-diphenol structure and most diphenol compounds show potent chain-breaking antioxidant activity in food systems (Shahidi *et al*, 1992). This molecule has antimicrobial activity (Oluwatuyi *et al*, 2004; Moreno *et al*, 2006), is able to inhibit lipid absorption in humans (Ninomiya *et al*, 2004) and is a free radical scavenger, due to its phenolic skeleton (Masuda *et al*, 2001, 2002; del Bano *et al*, 2003). In this study, we investigated the inhibitory effect of CA on TNF-α-induced HASMCs migration and MMP-9 activity.

In the present study, two polyphenolic compounds, Curcumin and CA, were examined for their effects on TNF-α-induced cell migration in HASMCs and also elucidate its possible mechanism.
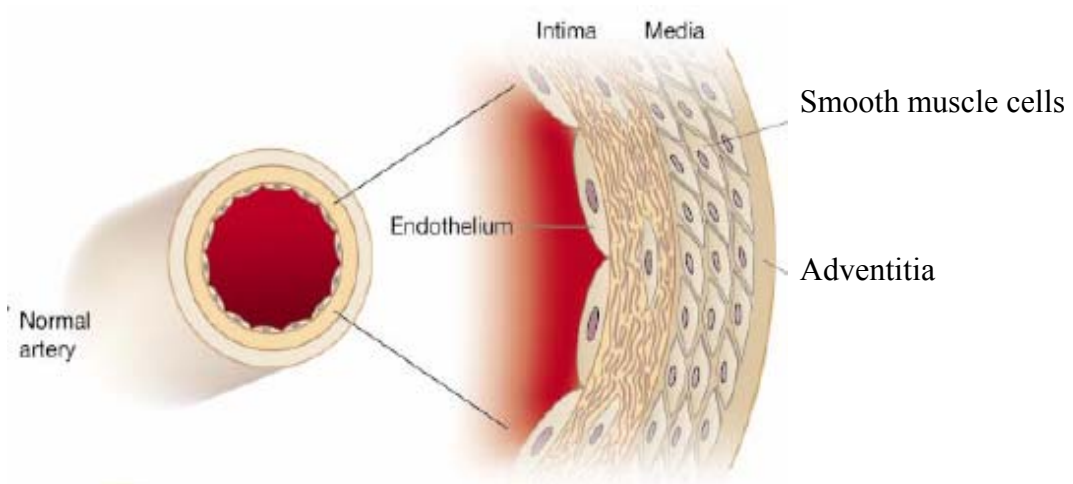
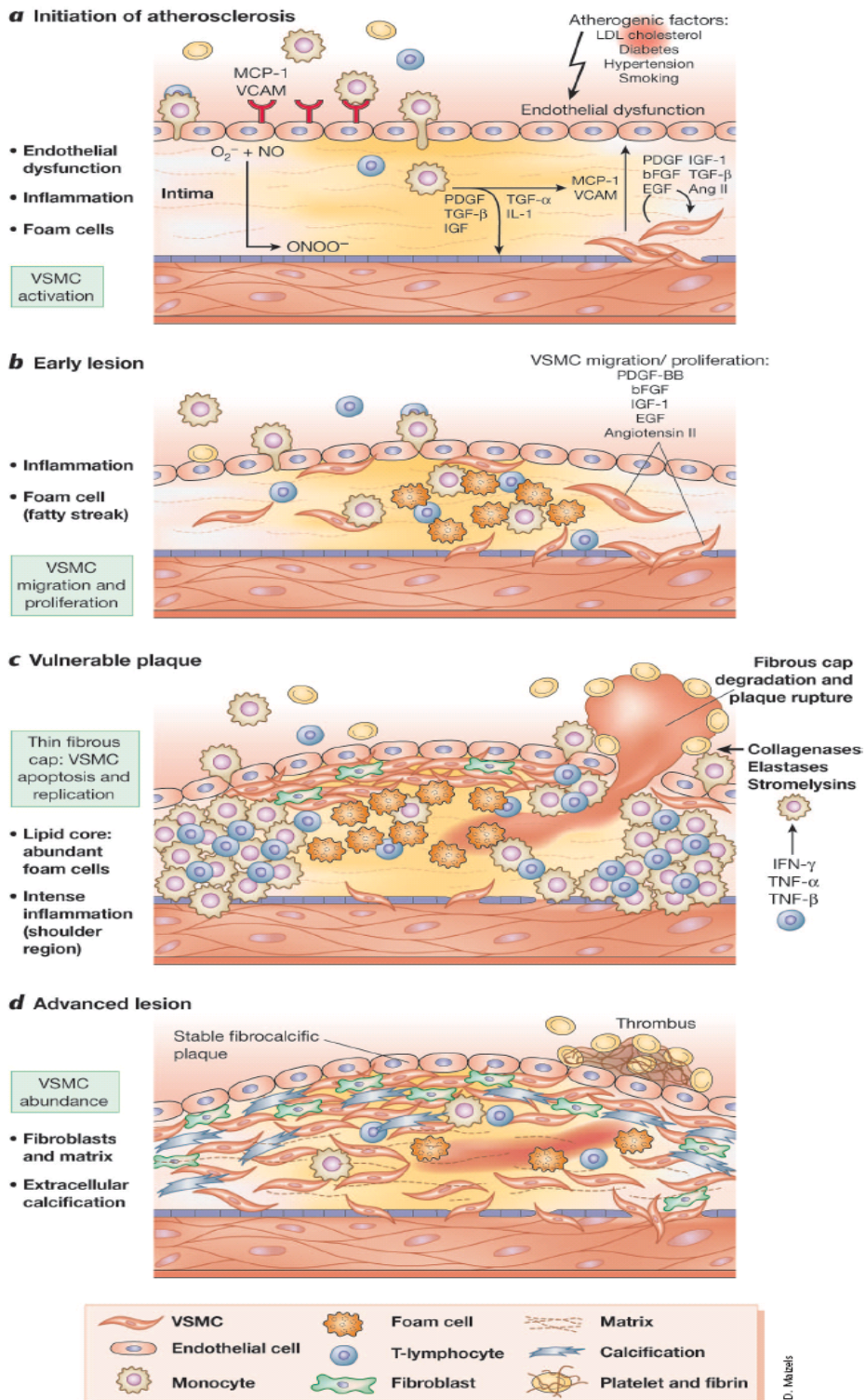Fig. 1. The structure of the normal blood wall. (Libby, 2002)

Fig. 2. The function of VSMCs during different stages of atherosclerosis. (Dzau *et al*, 2002)
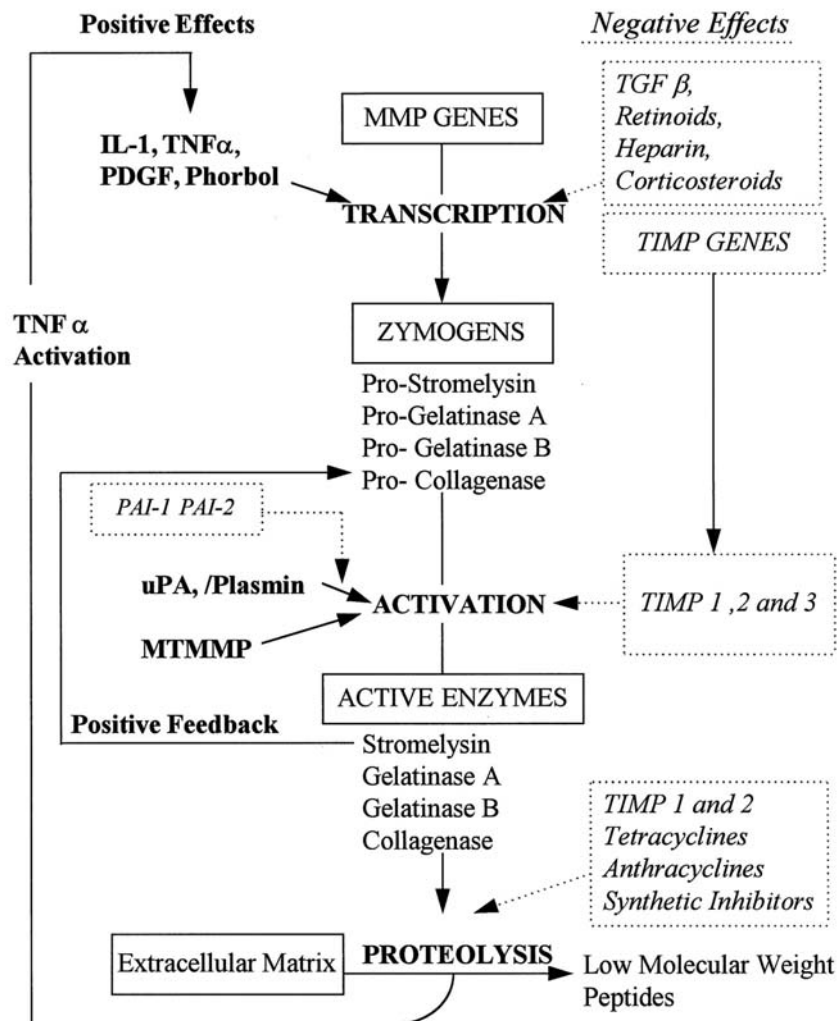
Fig. 3. The regulation of MMPs. (Dollery *et al*, 1995)

TABLE 1.   MMPs and Their Substrates

| Enzyme	MMP Classification	Substrate
Collagenases		
Interstitial collagenase	MMP-1	Collagens I, II, III, VII, and X, gelatin, entactin, aggrecan
Neutrophil collagenase	MMP-8	Collagens I, II, and III, aggrecan
Collagenase-3	MMP-13	Collagens I, II, and III, gelatin, fibronectin, laminins, tenascin
Collagenase-4[79]	MMP-18	Not known
Gelatinases		
Gelatinase A	MMP-2	Gelatin, collagens I, IV, V, VII, and X, fibronectin, laminins, aggrecan, tenascin-C, vitronectin
Gelatinase B	MMP-9	Gelatin, collagens IV, V, and XIV, aggrecan, elastin, entactin, vitronectin
Stromelysins		
Stromelysin 1	MMP-3	Gelatin, fibronectin, laminins, collagens III, IV, IX, and X, tenascin-C, vitronectin
Stromelysin 2	MMP-10	Collagen IV, fibronectin, aggrecan
Stromelysin 3	MMP-11	Fibronectin, gelatin, laminins, collagen IV, aggrecan
Membrane-type MMPs		
MT1-MMP	MMP-14	Collagens I, II, and III, fibronectin, laminins, vitronectin, proteoglycans; activates proMMP-2 and proMMP-13
MT2-MMP	MMP-15	Activates proMMP-2
MT3-MMP	MMP-16	Activates proMMP-2
MT4-MMP	MMP-17	Not known
MT5-MMP[80]	MMP-24	Activates proMMP-2
MT6-MMP	MMP-25	. . .
Others		
Matrilysin	MMP-7	Gelatin, fibronectin, laminins, collagen IV, vitronectin, tenascin-C, elastin, aggrecan
Metalloelastase	MMP-12	Elastin
Unnamed[81]	MMP-19	Not known
Enamelysin	MMP-20	Aggrecan
	MMP-23	. . .
Endometase	MMP-26	. . .

(Creemers *et al*, 2001)

16
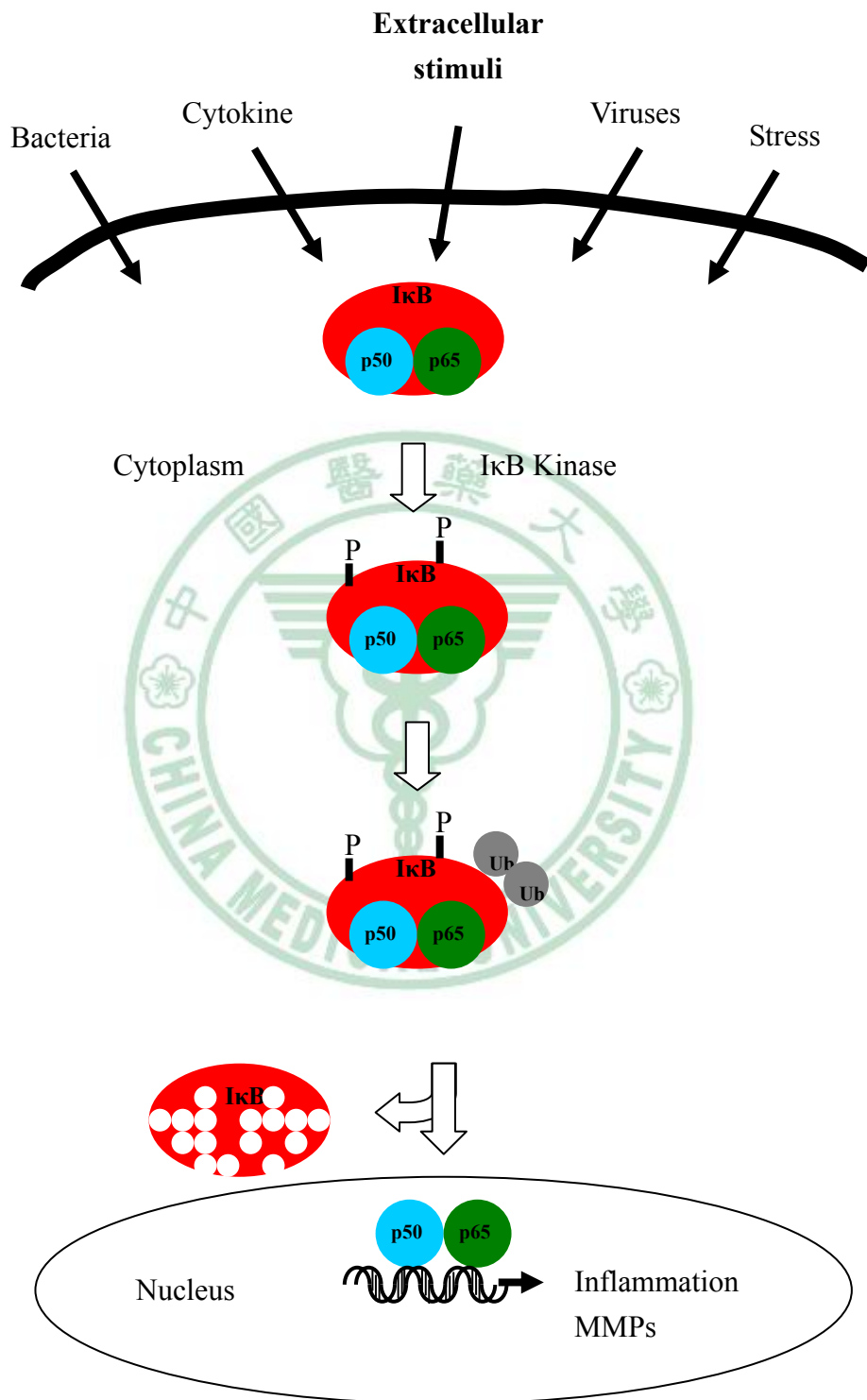
Fig. 4. The signal transduction pathways of NF-κB activation. (Martin *et al*, 2000)
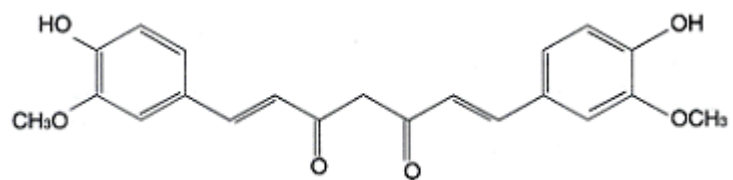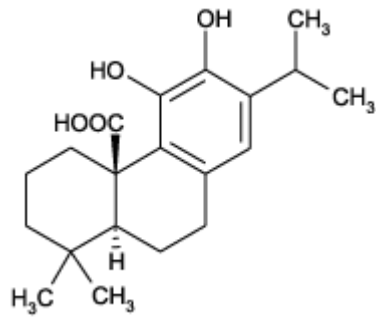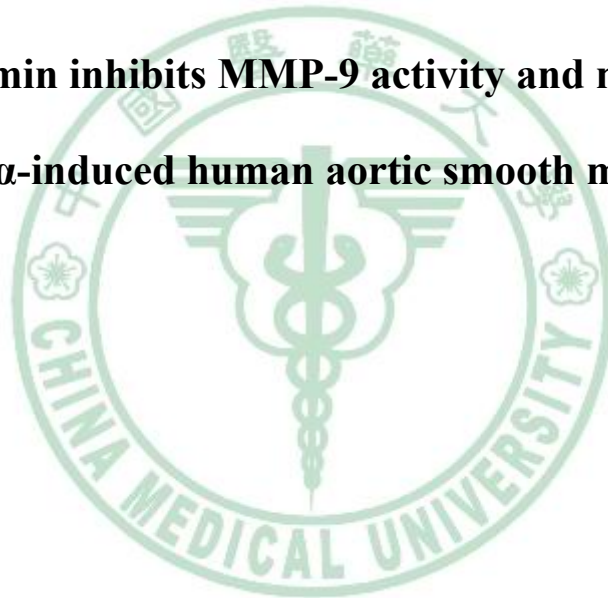
Fig. 5. The structure of curcumin.

Fig. 6. The structure of carnosic acid.

Chapter 2

薑黃素抑制細胞激素誘發人類大主動脈平滑肌細胞的遷移和

基質金屬蛋白酶的活化

Curcumin inhibits MMP-9 activity and migration of

TNF-α-induced human aortic smooth muscle cells

2.1 Introduction

Atherosclerosis, a progressive pathological disorder leading to cardiovascular and cerebrovascular diseases, is still the leading cause of mortality and morbidity in industrialized countries, in spite of improved pharmacological and lifestyle approaches (Ross, 1993). It is a chronic inflammatory disease driven by risk factors that cause oxidative and inflammatory mechanisms. Oxidative stress may lead to many cellular events, such as inactivation of NO, oxidative modifications of DNA and proteins, lipid oxidation, enhanced mitogenicity and apoptosis of vascular cells, and increased expression and activation of redox-sensitive genes, such as the receptor for oxidized LDL, adhesion molecules, chemotaxis factors, proinflammatory cytokines, regulators of cell cycle progression, and matrix metalloproteinases (Wassmann *et al*, 2004). Previous studies also indicated that proinflammatory cytokines, such as tumor necrosis factor (TNF) and interleukin-1 (IL-1), play an important role in the pathogenesis of atherosclerosis (Zhu *et al*, 1999; Rahman *at al*, 1998).

The migration of SMCs from the tunica media to the subendothelial region is a key event in the development and progression of many vascular diseases including atherosclerosis and post-angioplasty restenosis (Maeda *et al*, 2002). MMPs activity may contribute to the pathogenesis of atherosclerosis by facilitating migration of vascular smooth muscle cells (VSMCs) (Jones *et al*, 2003). MMPs (MMP-9 and MMP-2) production and SMCs migration may play key roles in the pathogenesis of neointima formation and atherosclerosis. The activity of the 92 kDa (MMP-9) but not the 72 kDa (MMP-2) gelatinase is induced by IL-1α, TNF-α and phorbol esters, in a

variety of cell types (Birkedal-Hansen *et al*, 1993; Fabunmi *et al*, 1996).

Transcription factor NF-κB and its target genes are involved in the pathogenesis of atherosclerosis (Kutuk and Basaga, 2003). NF-κB subunits form homo- and heterodimers, the most prominent one is p50/p65 heterodimers. The dimmer is retained in the cytoplasm in an inactive state through interaction with IκB. NF-κB is rapidly activated in response to a variety of inflammatory and other stimuli that lead to degradation of IκB (Martin *et al*, 2000). Upon activation of NF-κB, a large number of genes are induced including various inflammatory cytokines, adhesion molecules, and MMPs (Baeuerle, 1991; Grilli *et al*, 1993; Martin *et al*, 2000).

Curcumin, which is consumed daily by millions of people, is a polyphenol derived from the plant *Curcuma longa*. In general, curcumin has been associated with a large number of biological and cellular activities, including antioxidative, anti-inflammatory, anticarcinogenic, and hypocholesterolemic properties (Gafner *et al*, 2004; Shishodia *et al*, 2005; Aharma *et al*, 2005; Aggarwal and Shishodia, 2006; Maheshwari *et al*, 2006). In this study, we investigated the inhibitory effect of curcumin on TNF-α-induced human aortic smooth muscle cells (HASMCs) migration and MMP-9 activity.

2.2 Materials and Methods

2.2.1 Materials

2.2.1.1 Instruments

CO_2 incubator	NUAIRE, MN, USA
Laminar flow	NUAIRE, MN, USA
Microscope	Nikon, Japan
pH meter	HANNA, RI, USA
Stirrer/Hotplate	Corning, Taiwan
Waterbath tank	TKS, Taiwan
Haemocytometer	Boeco, Germany
Eppendorf centrifugator	Hamburg, Germany
Pipetman	Gilson, France
Spectrophotometer	HITACHI, Japan
Spectrophotometer	Beckman Coulter, CA, USA
MicroPlate fluorescence reader	Bio-Tek, VT, USA
Shaking incubator	Orbital, VA, USA
ELISA plate reader	Bio-Tek, VT, USA
Electrophoresis tank	Bio-Rad, CA, USA
Transfer system	Bio-Rad, CA, USA

Electrophoresis chamber   Bio-Rad, CA, USA

Power supply   Hoefer, CA, USA

2.2.1.2 Chemicals

40 % Acrylamide   Amresco, OH, USA

2, 7-dichlorofluorescein diacetate (DCFH-DA)   Molecular Probe, OR, USA

3-(4, 5-dimethylthiazol-2-yl)-2, 5-diphenyl tetrazolium bromide (MTT)

        Sigma, MO, USA

Acetic acid   Amresco, OH, USA

Bovine serum albumin (BSA)   Sigma, MO, USA

Bradford   Bio-Rad, CA, USA

Chloroform   BDH, Poole, England

Curcumin   Sigma, MO, USA

Diethyl pyrocarbonate (DEPC)   Sigma, MO, USA

Dimethyl sulfoxide (DMSO)   Amresco, OH, USA

Dodecylsulfate sodium salt (SDS)   Amresco, OH, USA

Enhanced chemiluminescence (ECL)   Upstate, CA, USA

Ethanol   景明化工, Taichung, Taiwan

F12K   Sigma, MO, USA

Fetal bovine serum (FBS)   Gibco, NY, USA

Gelatin   Amresco, OH, USA

Glycerol   Amresco, OH,USA

Glycine   Amresco, OH, USA

Hepes	Gibco, NY, USA
Invasion assay kit	Chemicon, CA, USA
Isopropanol	Sigma, MO, USA
Methanol	Tedia, OH, USA
Nuclear extract kit	TransAM, CA, USA
NF-κB kit	TransAM, CA, USA
Penicillin-Streptomycin	Gibco, NY, USA
Recombinant human TNF-α	Cytolab, Rehovot, Israel
Sodium biocarbonate	Sigma, MO, USA
Sodium chloride	Sigma, MO, USA
Temed	Amresco, OH, USA
Tris base	Amresco, OH, USA
Tris-HCl	Amresco, OH, USA
Triton X-100	Amresco, OH, USA
Trizol	Invitrogen, CA, USA
Trypsin	Sigma, MO, USA
Trypan blue	Sigma, MO, USA
Tween-20	Amresco, OH, USA

2.2.1.3 Antibodies

Primary antibodies

Mouse anti-human β-actin	Abcam, Cambridge, UK
Rabbit anti-human matrix metallproteinases-9	Abcam, Cambridge, UK

Secondary antibodies

Sheep anti-mouse IgG antibody   Abcam, Cambridge, UK

Goat anti-rabbit IgG antibody   Abcam, Cambridge, UK

2.3 Methods

2.3.1 Cell culture

Human aortic smooth muscle cells (HASMCs) were purchased from Food Industry Research and Development Institute, 新竹, Taiwan (CCRC 60293). They were maintained in Ham's F12K containing 10 % fetal bovine serum, 2 mmol/l L-glutamine, 1.5 g/l sodium bicarbonate, 10 mmol/l HEPES, 10 mmol/l TES, 0.05 mg/ml ascorbic acid, 0.01 mg/ml transferrin, 0.01 mg/ml insulin, 10 ng/ml sodium selenite, 0.03 mg/ml ECGs. All experiments were performed with HASMCs from passages 21 to 31, which were grown to 80-90 % confluence and made quiescent by serum starvation (0.1 % FBS) for at least 24 h.

2.3.2 Cell viability assay (MTT assay)

The cytotoxic effect of curcumin on HASMCs was investigated using 3-(4, 5-dimethylthiazol-2-yl)-2, 5-diphenyl tetrazolium bromide (MTT) assay (Chen *et al*, 2002). The principle of this assay is that mitochondria dehydrogenase in viable cells reduces MTT to a blue formazan. Briefly, the cells were grown in 96-well culture plates at a density of 1×10^4 cells per well in F-12K culture medium and incubated with various concentrations of curcumin for 24 hours. 10 μl MTT (5 mg/ml) were then added to each well and incubation continued at 37 °C for an additional 4 hours. The medium was then carefully removed, so as not to disturb the formazan crystals which had formed. Dimethyl sulphoxide (100 μl), which solubilizes formazan crystals, was

added to each well and absorbance of the solubilized blue formazan was measure the optical density at 590 nm using µQuant Microplate Spectrophotometer (Bio-Tek, VT, USA). All determinations were performed according to three individual experiments. The data were shown mean±SD as percentage of control.

2.3.3 Gelatin zymography for MMP-9

MMP-9 activity in conditioned medium of cultured HASMCs was analyzed by substrate-gel electrophoresis (zymography) using SDS-PAGE (10 %) containing 0.1 % gelatin. Substrate gel zymography of the activity of MMP-9 was performed with a Mini-Protein II apparatus from Bio-Rad, according to a method described previously (Demeule *et al*, 2000). Cells were grown to sub-confluence and were rinsed with phosphate-buffered saline (PBS) and then incubated in serum-free medium for 24 h. Equal volumes of samples of conditioned cell culture medium were mixed with sample buffer containing 62.5 mmol/l Tris-HCl (pH 6.8), 10 % glycerol, 2 % SDS, and 0.00625 % (w/v) bromophenol blue, loaded onto the gel and separated by electrophoresis. Thereafter, gels were washed 3 times for 30 minutes at room temperature in buffer (50 mmol/l Tris-HCl, pH 8.0, 5 mmol/l $CaCl_2$, 0.02 % NaN_3, and 2.5 % Triton X-100) and incubated for 18 h at 37 °C with the same buffer except Triton X-100. Gels were stained with Coomasssie Brillant Blue R-2500 (0.1 %) and destained in 5 % methanol and 7 % acetic acid. Gelatinolytic activity appeared as a clear band on a blue background.

2.3.4 Bradford protein assay

The Bradford assay (Bradford, 1976), a colorimetric protein assay, is based on an absorbance shift in the dye Coomassie when bound to arginine and hydrophobic amino acid residues present in protein. The anionic (bound) form of the dye is blue and has an absorption spectrum maximum historically held to be at 595 nm. The cationic (unbound) forms are green and red. The increase of absorbance at 595 nm is proportional to the amount of bound dye, and thus to the amount (concentration) of protein present in the sample. Standard solutions contain a range of 0 to 25 micrograms protein (BSA) in 800 µl H_2O, followed by adding 200 µl dye reagent and incubate 5 min. l µl of sample solution add into 799 µl H_2O, followed by adding 200 µl dye reagent and incubated for 5 min. The absorbance was read at 595 nm. The results made a standard curve and the protein concentration of sample was determined by standard curve.

2.3.5 Western blot analysis

HASMCs were treated with various concentrations of curcumin in the presence of 100 ng/ml TNF-α. Cellular lysates were prepared in a lysis buffer containing 10 mmol/l Tris/HCl (pH 8), 0.32 mol/l sucrose, 5 mmol/l Ethyienediamine Teraacetate Disodium Salt (EDTA), 1 % Triton X-100, 2 mmol/l 1, 4-Dithio-D,L-thereitol (DTT), 1 mmol/l PMSF. The cells were disrupted and extracted at 4 °C for 30 min. After centrifugation at 13,000 rpm for 15 min, the supernatant was obtained as the cell lysate. Protein concentrations were measured using the bradford assay. Total protein (20 µg) were subjected to SDS-PAGE (10 %) and blotted on PVDF membranes (Shishodia *et al*, 2003). Nonspecific binding was blocked by soaking the membrane in PBS-Tween

20 (PBST) buffer containing 50 g/l nonfat milk. The membrane was incubated with monoclonal mouse anti-human β-actin (1:1000) and polyclonal rabbit anti-human MMP-9 (1:1000). Subsequently, the membrane was incubated with sheep anti-mouse IgG antibody (1:5000) and goat anti-rabbit IgG antibody (1:5000). The protein levels were determined using the enhanced chemiluminescence detection reagents (Upstate, CA, USA) and high performance chemiluminescence film (Amersham, IL, USA). Incubation with mouse anti-human β-actin antibody was also performed as an internal control. Results were quantified with scanning densitometer using an image analysis system with software.

2.3.6 Preparation of nuclear extract

Nuclear protein extracts of HASMCs were prepared using a nuclear extract kit (TransAM nuclear extract kit, CA, USA). Cells were lysed in hypotonic buffer and centrifuge suspension for 30 seconds at 14,000×g in a microcentrifuge pre-cooled at 4 °C (Dschietzig *et al*, 2001). Then resuspend nuclear pellet in 50 μl complete lysis buffer containing 10 mmol/l DTT, lysis buffer AM2, and protease inhibitor cocktail by pipetting up and down. The suspension was incubated for 30 min on ice, and centrifuged for 10 min at 14,000×g in a microcentrifuge pre-cooled at 4 °C. Transfer supernatant and stored at -80 °C. Protein concentrations were measured using the bradford protein assay.

2.3.7 ELISA-Based Nuclear Factor-κB Assay

Additionally to gel-shift assays, an ELISA-based kit was used for quantitative detection of NF-κB activity (TransAM NF-κB kit, CA, USA). For each sample, 20 μl of nuclear extracts (5 μg protein) were used according to the instructions of the manufacturer (Yu *et al*, 2007). Nuclear extracts were incubated with the oligonucleotide-coated wells for 60 min. Where indicated a competitor for NF-κB binding (NF-κB wild-type consensus oligonucleotide) was added in molar excess prior to the probe. The wells were then washed and incubated with the primary antibodies for p50 and p65 for 60 min. After incubation with a horseradish peroxidase-conjugated secondary antibody, a substrate was added to produce blue colour and then for quantitation by μQuant Microplate Spectrophotometer (Bio-tek, VT, USA). The absorbance was read at 590 nm and the blank was subtracted from all measurements.

2.3.8   Cell migration assay

VSMCs invasion through the extracellular matrix was determined by using a commercial cell invasion assay kit (Chemicon, CA, USA). HASMCs (1.5×10^5 cells/300 μl) were resuspended in conditioned medium collected from pretreatment with curcumin and TNF-α-treated cells for 23 hours, and added to the upper components of migration chamber (Bedoui *et al*, 2005). Five hundred microliters of same conditioned medium were added to the lower compartment of migration chamber. Cells without TNF-α-treated conditioned medium served as control. The migration chambers were incubated at 37 °C for 24 hours in 5 % CO_2. After incubation, the inserts were removed from the wells, and the cells on the upper side of the filter were removed using cotton swabs. The filters were fixed, and stained according to the

manufacturer's instructions. The cells that invaded and were located on the underside
of the inserts. Then transfer 100 µl of the dye mixture to a 96-well plate, and measure
the optical density at 560 nm.
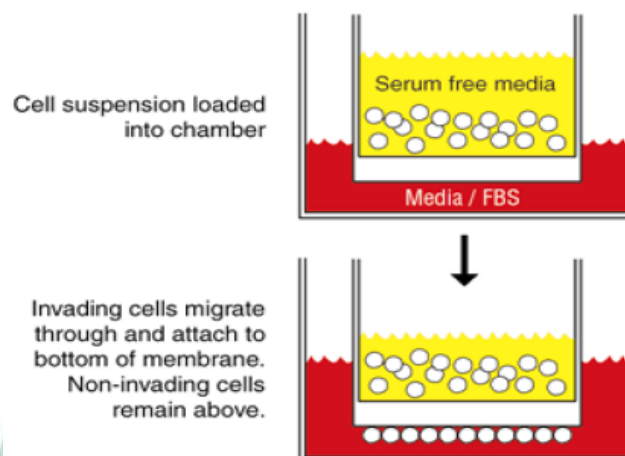
2.3.9 Measurement of intracellular ROS

HASMCs were pretreated with 10 and 20 µmol/l curcumin for 1 hour and
induced by TNF-α (100 ng/ml) for 23 hours. Then were incubated with 10 µmol/l
2,7-dichlorofluorescein (DCF) diacetate (DCFH-DA) for 30 minutes, which is
converted to DCF by intracellular esterase (Kim *et al*, 2006). The latter was then
oxidized by ROS to the highly fluorescent DCF. The fluorescence of each dish was
immediately analyzed at excitation wavelength of 485 nm and emission wavelength of
528 nm by FLx800 microplate fluorescence reader (Bio-tek, VT, USA). All
measurements were at least triplicated.

2.3.10 Statistical analysis

Results are shown as mean±SD. Statistical analyses of MTT were performed using One-way ANOVA followed by Dunnett's test and others were performed using One-way ANOVA followed by Duncan's Multiple Range Test. A value of $p<0.05$ was considered statistically significant.

2.4 Results

2.4.1 Cytotoxicity of curcumin on HASMCs.

The cytotoxity of curcumin on HASMCs were evaluated using MTT assay. The HASMCs (1×10^4 cells/well) were incubated for 24 h in cultures in 96-well with various concentrations of curcumin (0, 10, 20, 30, 50, and 75 μmol/l). Dose-dependent cytotoxic effect of curcumin against HASMCs was shown in Fig. 2-1 (100 %, 92±0.5 %, 91.2±0.8 %, 84.8±4.2 %, 81.8±6.5 %, and 67±13 %, respectively.). According to the MTT assay, we chose 10 and 20 μmol/l of curcumin to do all the following experiments.

2.4.2 Curcumin prevents TNF-α-induced activation of MMP-9 in HASMCs.

The inhibitory effect of curcumin on TNF-α-induced MMP-9 activation were analysed by gelatin zymography. HASMCs were pretreated with 10 and 20 μmol/l curcumin for 1 h, and then induced by TNF-α (100 ng/ml) for additional 23 h. As shown in Fig. 2-2, MMP-9 secretion was markedly induced by TNF-α, and suppressed by curcumin. The 20 μmol/l curcumin treatment is more effective on activation of MMP-9 than 10 μmol/l curcumin.

2.4.3 Curcumin suppresses TNF-α-induced MMP-9 expression in HASMCs.

The effect of MMP-9 expression by curcumin in HASMCs was assessed by Western blot. HASMCs were pretreated with 10 and 20 μmol/l curcumin for 1 h, and induced by TNF-α (100 ng/ml) for 23 h. MMP-9 expression was markedly induced by TNF-α, and suppressed by curcumin (Fig. 2-3). The 20 μmol/l curcumin treatment is more effective on protein expression of MMP-9 than 10 μmol/l curcumin.

2.4.4　Curcumin suppresses nuclear translocation of NF-κB p50 and p65 in TNF-α-induced HASMCs.

To determine whether the inhibitory effect of curcumin on the TNF-α-induced expression of MMP-9 is medicated via NF-κB, we measured the nuclear translocation of p50 and p65 of the NF-κB family. Treatment of TNF-α (100 ng/ml) for 23 h enhanced the nuclear translocation of p50 (Fig. 2-4) and p65 (Fig. 2-5). Pretreatment of HASMCs with 10 and 20 μmol/l curcumin prior to TNF-α stimulation did significantly prevent the nuclear translocation of p50 and p65. As shown in Fig. 2-4, the 20 μmol/l curcumin treatment is more effective on nuclear translocation of NF-κB p50 than 10 μmol/l curcumin. In Fig. 2-5, the 20 μmol/l curcumin treatment is more effective on decreased nuclear translocation of NF-κB p65 than 10 μmol/l curcumin.

2.4.5　Curcumin suppresses TNF-α-induced HASMCs migration.

HASMCs (1.5×10^5 cells/300 μl) were pretreated with 10 and 20 μmol/l curcumin for 1 hour, and induced by TNF-α (100 ng/ml) for 23 h. As shown in Fig. 2-6, the migration of HASMCs was increased by TNF-α stimulation. The stimulatory

effect of TNF-α was significantly reduced by curcumin pretreatment. The 20 μmol/l curcumin treatment is more effective on decreased HASMCs migration than 10 μmol/l curcumin.

2.4.6 Curcumin suppresses TNF-α-induced ROS generation.

To characterize the events underlying TNF-α-induced migration, we examined the generation of ROS after TNF-α treatment in HASMCs. HASMCs were exposed to TNF-α (100 ng/ml) for 23 h, and DCF fluorescence produced was measured (Fig. 2-7). The production of ROS was induced by TNF-α and decreased by curcumin. The 20 μmol/l curcumin treatment is more effective on reduced ROS generation than 10 μmol/l curcumin.
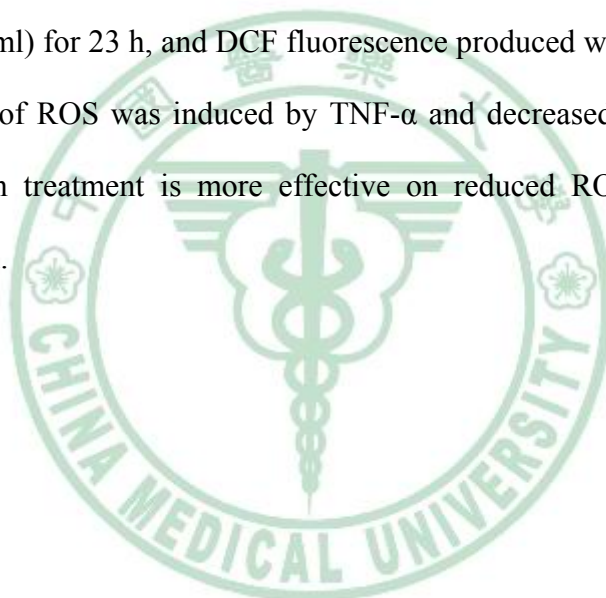
2.5 Discussion

In this study, we investigated the effect of curcumin on HASMCs migration and MMP-9 activation induced by TNF-α. Curcumin lowered the secretion and protein expression of MMP-9 by gelatin zymography and Western blot assays. It also decreased nuclear translocation of nuclear factor-κB (NF-κB) P50 and P65. In addition, the migration assay showed that curcumin effectively inhibited the TNF-α-induced migration of HASMCs as compared with the control group. In our *in vitro* study, we also found that curcumin could scavenge DPPH (2, 2-diphenyl-1-picrylhydrazyl) radicals, alkoxyl radical (RO˙), and peroxyl radical (ROO˙). It is approximately 2-3-folds more potent than Trolox in antioxidative ability (Appendix 1). It also could suppress TNF-α-induced intracellular ROS production.

Curcumin, which is consumed daily by millions of people, is a polyphenol derived from the plant Curcuma longa (Fang *et al*, 2005). It exhibits a variety of pharmacological effects including anti-tumor, anti-inflammtory, anti-infectious activities and is currently in clinical trials for AIDS patients (Mazumder *et al*,1995; Ruby *et al*, 1995; Surh, 2002). Commercial curcumin usually isolated from the rhizome of *Curcuma longa* Linn. which contain approximately 77 % of curcumin (Ahsan *et al*, 1994). Previous study indicated that the serum concentration was 1.77±1.87 μmol/l after 8 g curcumin intake in human (Cheng *et al*, 2001), therefore, curcumin was absorbable in digestive tract in human. In the present study, we found that 20 μmol/l of curcumin did not have any significant effect on the cytotoxity of HASMCs from MTT test. Therefore, we chose 10 and 20 μmol/l curcumin to do all

the experiments (Fig. 2-1).

The migration of SMCs from the tunica media to the subendothelial region is a key event in the development and progression of many vascular diseases including atherosclerosis and post-angioplasty restenosis (Maeda *et al*, 2002). MMPs (MMP-2 and MMP-9) activities may contribute to the pathogenesis of atherosclerosis by facilitating migration of VSMCs (Jones *et al*, 2003). Although MMP-2 and MMP-9 have similar substrate specificities, the regulation of their expression are different. MMP-2 is constitutively expressed by several cell types, including SMCs, and its expression is not induced by cytokines or growth factors. In contrast, MMP-9 can be induced by TNF-α in SMCs (Cho *et al*, 2000; Galis *et al*, 1994). Therefore, we have investigated the effect of curcumin on the migration of HASMCs and activation of MMP-9. The results indicated that the migration of HASMCs was significantly induced by TNF-α, and suppressed by curcumin (Fig. 2-6). This inhibition against TNF-α-induced migration of HASMCs is consistent with the inhibition of activation and expression of MMP-9 (Fig. 2-2 and Fig. 2-3). A similar result was seen when HASMCs were pretreated with other polyphenolic compound, such as tea flavonoid epigallocatechin-3-gallate (20 μmol/l), quercetin (40 μmol/l), and other flavonoids (Kim *et al*, 2005; Moon *et al*, 2003).

The NF-κB family controls the expression of genes involved in the inflammation and immune response (Baeuerle, 1991). In the cytoplasm, inactive NF-κB exists as a heterodimeric complex of subunits p50 and p65 that binds to a cytoplasmic protein, IκB (Baeuerle and Henkel, 1994). Upon activation, IκB is rapidly degraded, and the p50/p65 heterodimer is translocated from the cytoplasm into the nucleus where the dimmer interacts with regulatory κB elements in promoters and

enhancers, thereby controlling gene transcription (Baeuerle and Baltimore, 1988). NF-κB is activated by a multitude of stimuli, including various inflammatory cytokines and reactive oxygen intermediates (Baeuerle and Baltimore, 1998; Grilli *et al*, 1993; Muller *et al*, 1997), which are activated in atherosclerotic lesions (Brand *et al*, 1996). In the present study, curcumin reduced cytokine-induced nuclear translocation of p50 (Fig. 2-4) and p65 (Fig. 2-5) in HASMCs.

Much further work, which is beyond the scope of the present study, is necessary to elucidate the mechanisms underlying the synergistic regulation of MMP secretion by cytokines. We focused instead on defining the role played by the NF-κB transcription factor in the regulation of MMPs in HASMCs. A functional NF-κB site occurs in the proximal stimulatory region of the MMP-9 promoter (Sato and Seiki, 1993; Fini *et al*, 1994) and deletion of this site reduces upregulation of reporter gene constructs in response to cytokines. Until now, however it has been unclear what contribution NF-κB plays in the upregulation of the endogenous MMP-9 gene. Previous study has demonstrated that transient overexpression of IκBα in vascular SMCs only partially impaired upregulation of MMP-9, suggesting that NF-κB simply plays a permissive role in the upregulation of MMP-9 (Bond *et al*, 2001). In the present study, curcumin reduced cytokine-induced expression of MMP-9 and prevented the nuclear translocation of p50 (Fig. 2-4) and p65 (Fig. 2-5) in HASMCs. We suggested that inhibitory mechanisms of curcumin might interrupt a signaling cascade involving MMP-9 transcription-mediated activation of NF-κB.

Several studies have indicated that ROS are implicated in the activation of NF-κB (Muller *et al*, 1997). The current study shows that the ROS production stimulated by TNF-α was decreased by curcumin pretreatment in HASMCs (Fig. 2-7).

Based on this result, we proposed that the inhibitory effect of curcumin on MMP-9 expression and NF-κB activation may be due to its antioxidant and anti-inflammatory properties. In our *in vitro* study, we also found that curcumin could scavenge DPPH (2, 2-diphenyl-1-picrylhydrazyl) radicals, alkoxyl radical (RO$^{\bullet}$), and peroxyl radical (ROO$^{\bullet}$) (Table 2-1). It is approximately 2-3-folds more potent than Trolox in antioxidative ability (Appendix 1). Since atherosclerosis is a chronic inflammatory disease associated with increased oxidative stress in the VSMCs, it would be conceivable that the anti-atherogenic effects of curcumin might due to its antioxidative and anti-inflammatory properties. The inhibition of cytokine-induced MMP-9 expression has been described for other substances with anti-inflammatory properties such as tea flavonoid epigallocatechin-3-gallate, quercetin, and other flavonoids (Kim *et al*, 2005; Moon *et al*, 2003).
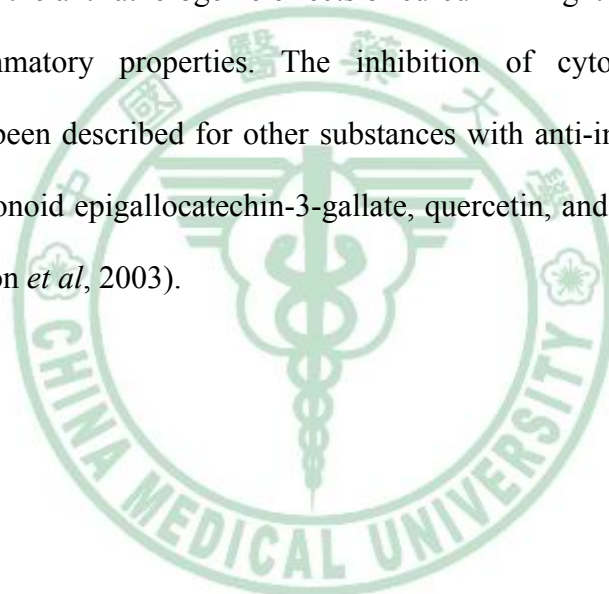
2.6 Conclusion

In this study, curcumin effectively inhibited the TNF-α-induced migration of HASMCs as compared with the control group. The ROS production, MMP-9 secretion and expression, nuclear translocation of NF-κB p50 and p65 were reduced by curcumin pretreatment. These results led us to conclude that curcumin could restrict the migration of HASMCs by suppressing MMP-9 through down-regulation of NF-κB.
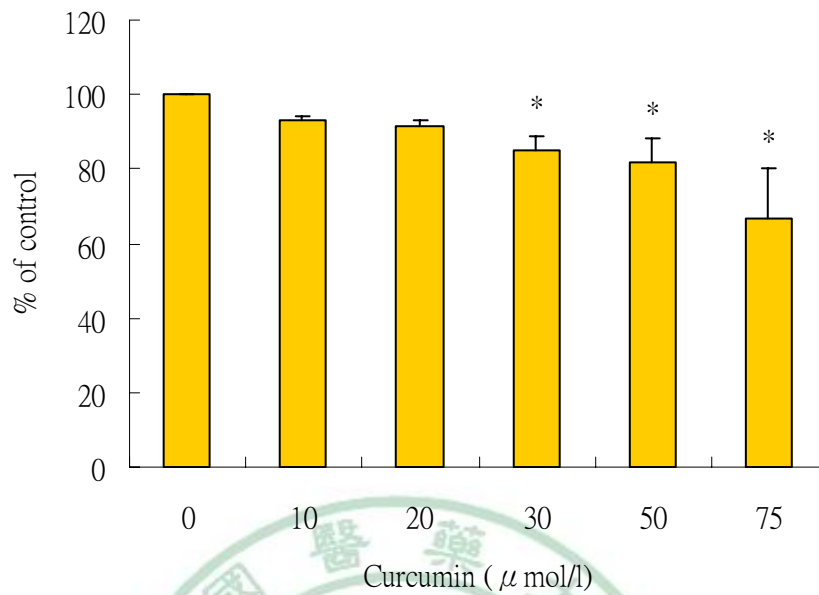
Fig. 2-1. Cytotoxic effect of curcumin on human aortic smooth muscle cells (HASMCs) with MTT test. HASMCs were treated with increasing concentrations (10~75 μmol/l) of curcumin for 24 h in 10 % FBS-F12K. Statistical analyses of MTT were performed using One-way ANOVA followed by Dunnett's test; n=3. *$p<0.05$ compared with control.
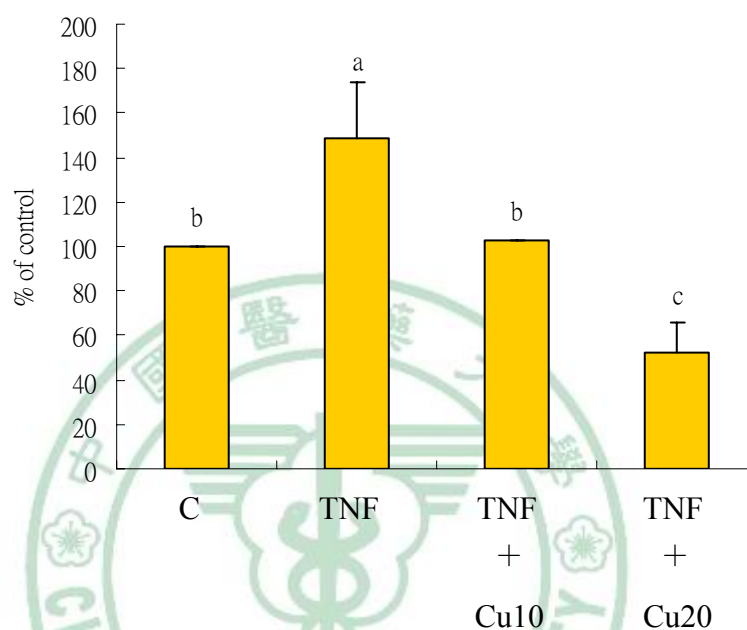
(A)

MMP-9

(B)

Fig. 2-2. Effect of curcumin on the MMP-9 activity of TNF-α-induced human aortic smooth muscle cells (HASMCs). HASMCs were pretreated with 10 and 20 μmol/l curcumin for 1 h, and induced by TNF-α (100 ng/ml) for additional 23 h. The activation of MMP-9 was assessed by gelatin zymography (A). Densitometric analysis was conducted with image analysis system software to quantify gelatin zymography data (B). Values are mean±SD, n=3. [a-c]Means with different letters are significantly different compared at $p<0.05$. Abbreviation: C (control without TNF-α or curcumin), TNF (TNF-α), Cu10 (curcumin 10 μmol/l), Cu20 (curcumin 20 μmol/l).

(A)

MMP-9

β-actin

(B)

Fig. 2-3. Curcumin inhibits the protein expression of MMP-9 in human aortic smooth muscle cells (HASMCs). HASMCs were pretreated with 10 and 20 μmol/l curcumin for 1 h, and induced by TNF-α (100 ng/ml) for additional 23 h. The expression of MMP-9 was assessed by western blot analysis. Representative western blot showing MMP-9 protein levels in cell lysates (top) and β-actin (bottom) (A). Densitometric analysis was conducted with image analysis system software to quantify western blot data (B). Values are mean±SD, n=3. [a-c]Means with different letters are significantly different compared at $p<0.05$. Abbreviation: C (control without TNF-α or curcumin), TNF (TNF-α), Cu10 (curcumin 10 μmol/l), Cu20 (curcumin 20 μmol/l).
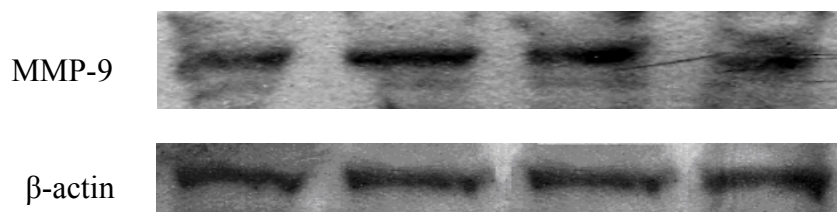
Fig. 2-4. Effect of curcumin on TNF-α-induced activation of NF-κB p50 in human aortic smooth muscle cells (HASMCs). HASMCs were pretreated with 10 and 20 μmol/l curcumin for 1 h and induced by TNF-α (100 ng/ml) for 23 h. Nuclear extracts were prepared and analyzed for activation of NF-κB family. Five micrograms of nuclear protein was used in each experiment. Values are mean±SD, n=3. [a-d]Means with different letters are significantly different compared at $p<0.05$. Abbreviation: C (control without TNF-α or curcumin), TNF (TNF-α), Cu10 (curcumin 10 μmol/l), Cu20 (curcumin 20 μmol/l).

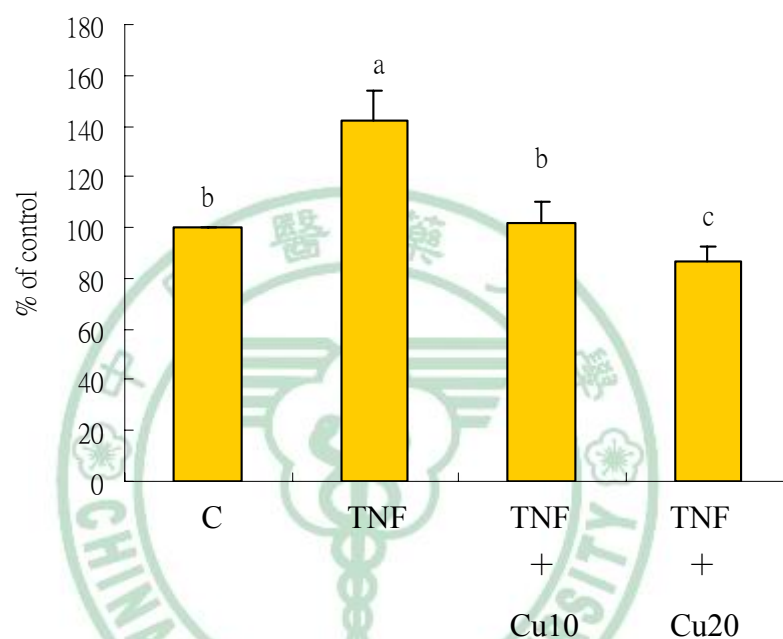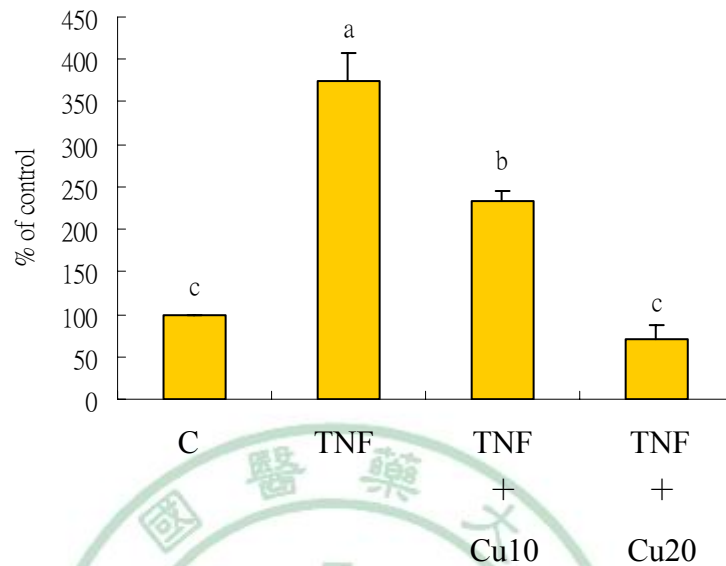Fig. 2-5. Effect of curcumin on TNF-α-induced activation of NF-κB p65 in human aortic smooth muscle cells (HASMCs). HASMCs were pretreated with 10 and 20 μmol/l curcumin for 1 h and induced by TNF-α (100 ng/ml) for 23 h. Nuclear extracts were prepared and analyzed for activation of NF-κB family. Five micrograms of nuclear protein was used in each experiment. Values are mean±SD, n=3. [a-d]Means with different letters are significantly different compared at $p<0.05$. Abbreviation: C (control without TNF-α or curcumin), TNF (TNF-α), Cu10 (curcumin 10 μmol/l), Cu20 (curcumin 20 μmol/l).

(A)

(a)

(b)

(c)

(d)
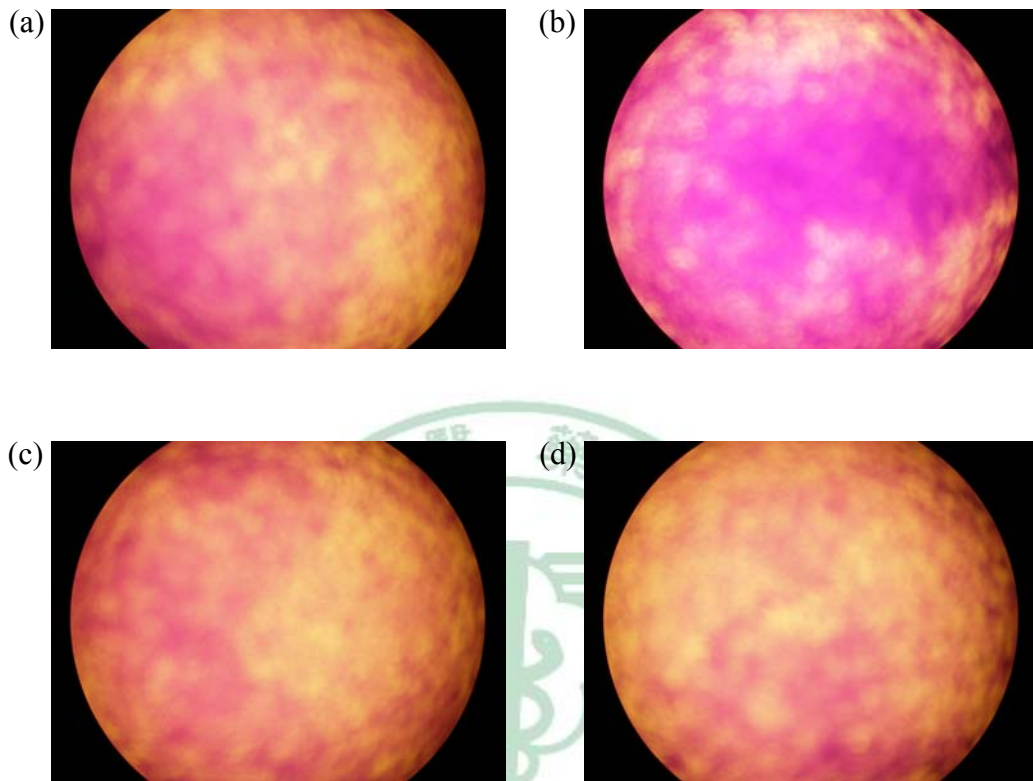
(B)

Fig. 2-6. Effect of curcumin on migrarion of human aortic smooth muscle cells (HASMCs) induced by TNF-α treatment. (A) Microphotographs of migrated cells without TNF-α or curcumin (a), with TNF-α (100 ng/ml) (b), with TNF-α (100 ng/ml) and 10 μmol/l of curcumin (c), and with TNF-α (100 ng/ml) and 20 μmol/l of curcumin (d) were captured. (B) HASMCs (1.5×10^5 cells/300 μl) were resuspended in conditioned medium collected from TNF-α treated cells for 23 h, and added to the upper components of migration chamber in the presence of 10 and 20 μmol/l curcumin. Values are mean±SD, n=3. [a-c]Means with different letters are significantly different compared at $p < 0.05$. Abbreviation: C (control without TNF-α or curcumin), TNF (TNF-α), Cu10 (curcumin 10 μmol/l), Cu20 (curcumin 20 μmol/l).
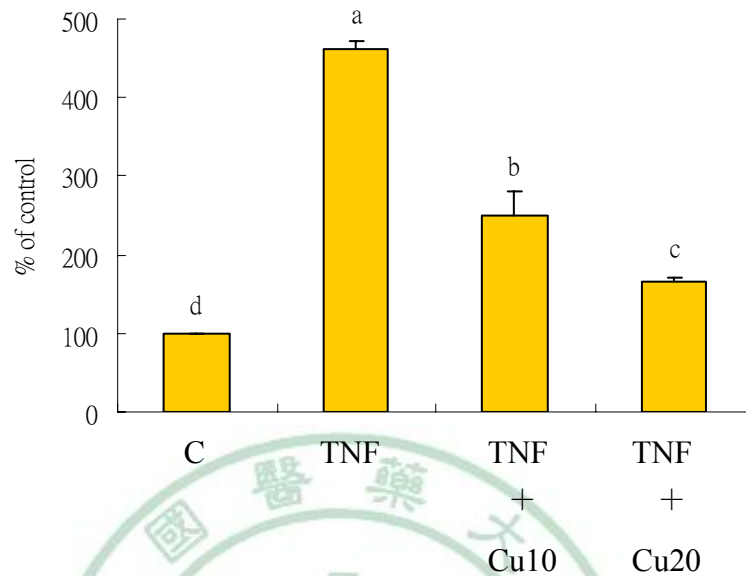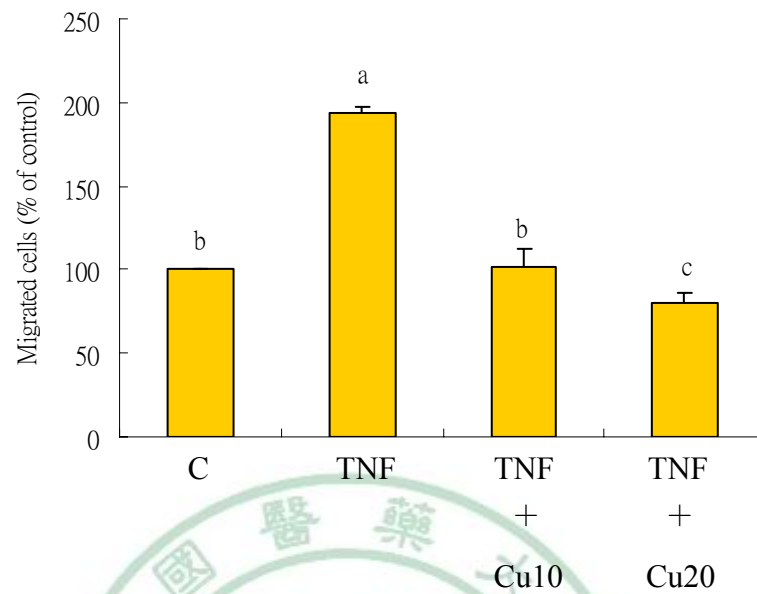
(A)

(a)

(b)

(c)

(d)
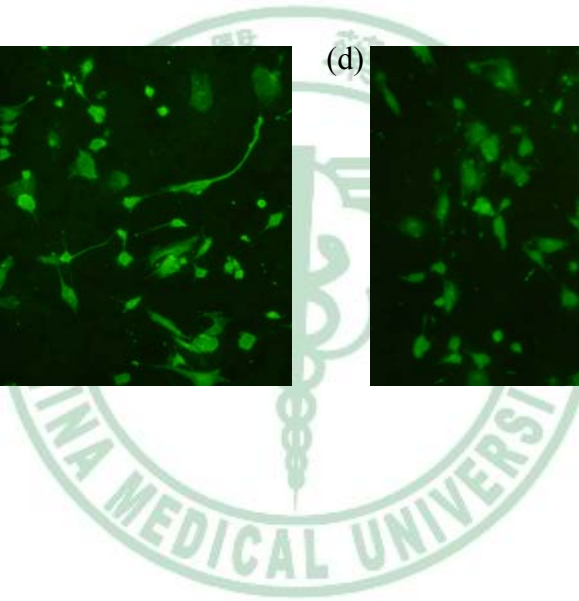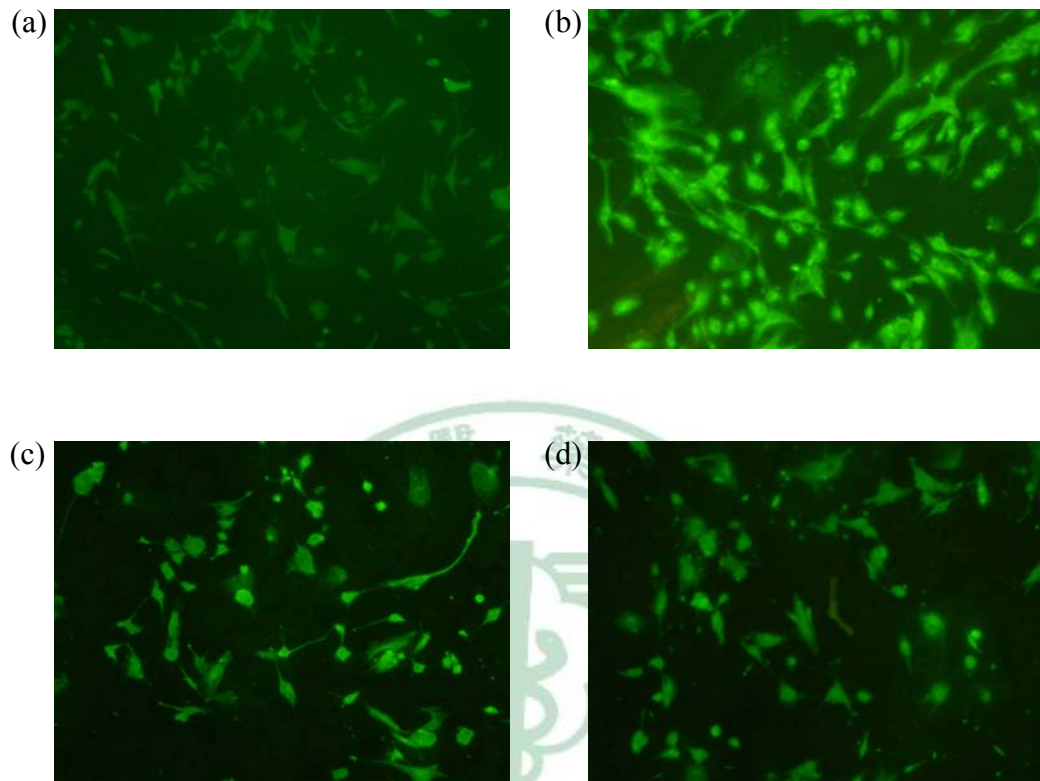
(B)
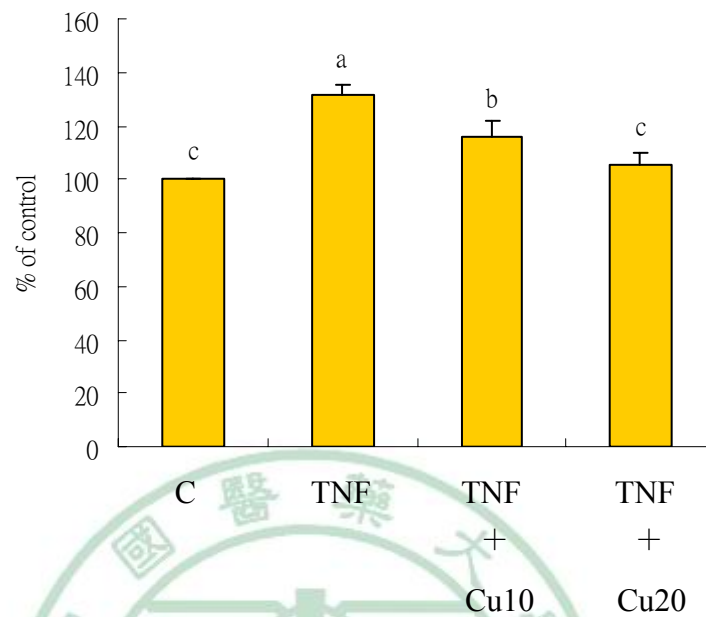
Fig. 2-7. Effect of curcumin on TNF-α-induced ROS production in human aortic smooth muscle cells (HASMCs). (A) Microphotographs of ROS production in HASMCs without TNF-α or curcumin (a), with TNF-α (100 ng/ml) (b), with TNF-α (100 ng/ml) and 10 μmol/l of curcumin (c), and with TNF-α (100 ng/ml) and 20 μmol/l of curcumin (d) were captured. (B) HASMCs were pretreated with 10 and 20 μmol/l curcumin for 1 h and induced by TNF-α (100 ng/ml) for 23 h. Values are mean±SD, n=3. [a-c]Means with different letters are significantly different compared at $p<0.05$. Abbreviation: C (control without TNF-α or curcumin), TNF (TNF-α), Cu10 (curcumin 10 μmol/l), Cu20 (curcumin 20 μmol/l).
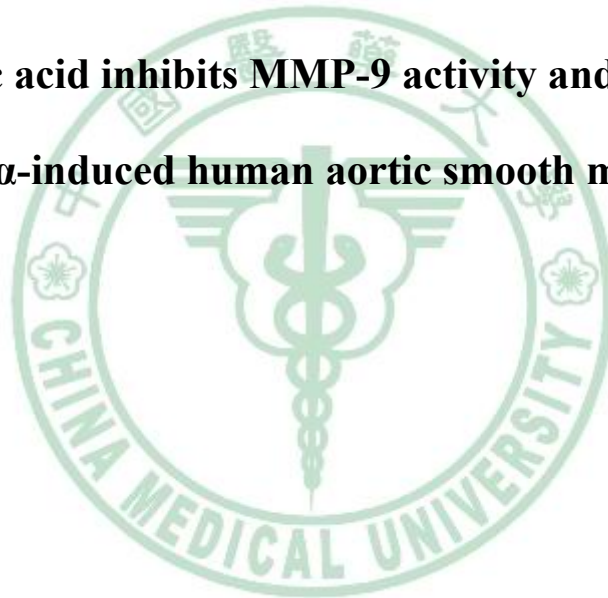
Chapter 3

鼠尾草酸抑制細胞激素誘發人類大主動脈平滑肌細胞的遷移

和基質金屬蛋白酶的活化

Carnosic acid inhibits MMP-9 activity and migration of

TNF-α-induced human aortic smooth muscle cells

3.1   Introduction

Atherosclerosis, a progressive pathological disorder leading to cardiovascular and cerebrovascular diseases, is still the leading cause of mortality and morbidity in industrialized countries, in spite of improved pharmacological and lifestyle approaches (Ross, 1993). It is a chronic inflammatory disease driven by risk factors that cause oxidative and inflammatory mechanisms. Oxidative stress may lead to many cellular events, such as inactivation of NO, oxidative modifications of DNA and proteins, lipid oxidation, enhanced mitogenicity and apoptosis of vascular cells, and increased expression and activation of redox-sensitive genes, such as the receptor for oxidized LDL, adhesion molecules, chemotaxis factors, proinflammatory cytokines, regulators of cell cycle progression, and matrix metalloproteinases (Wassmann *et al*, 2004). Previous studies also indicated that proinflammatory cytokines, such as tumor necrosis factor (TNF) and interleukin-1 (IL-1), play an important role in the pathogenesis of atherosclerosis (Zhu *et al*, 1999; Rahman *at al*, 1998).

The migration of SMCs from the tunica media to the subendothelial region is a key event in the development and progression of many vascular diseases including atherosclerosis and post-angioplasty restenosis (Maeda *et al*, 2002). MMPs activity may contribute to the pathogenesis of atherosclerosis by facilitating migration of VSMCs (Jones *et al*, 2003). MMPs (MMP-9 and MMP-2) production and SMCs migration may play key roles in the pathogenesis of neointima formation and atherosclerosis. The activity of the 92 kDa (MMP-9) but not the 72 kDa (MMP-2) gelatinase is induced by IL-1α, TNF-α and phorbol esters, in a variety of cell types

(Birkedal-Hansen *et al*, 1993; Fabunmi *et al*, 1996).

Transcription factor NF-κB and its target genes are involved in the pathogenesis of atherosclerosis (Kutuk and Basaga, 2003). NF-κB subunits form homo- and heterodimers, the most prominent one is p50/p65 heterodimers. The dimmer is retained in the cytoplasm in an inactive state through interaction with IκB. NF-κB is rapidly activated in response to variety of inflammatory and other stimuli that lead to degradation of IκB (Martin *et al*, 2000). Upon activation of NF-κB, a large number of genes are induced including various inflammatory cytokines, adhesion molecules, and MMPs (Baeuerle, 1991; Grilli *et al*, 1993; Martin *et al*, 2000).

CA is the primary phenolic compound in rosemary and salvia. Previous study indicated that CA has a typical *O*-diphenol structure and most diphenol compounds show potent chain-breaking antioxidant activity in food systems (Shahidi *et al*, 1992). This molecule has antimicrobial activity (Oluwatuyi *et al*, 2004; Moreno *et al*, 2006), is able to inhibit lipid absorption in humans (Ninomiya *et al*, 2004) and is a free radical scavenger, due to its phenolic skeleton (Masuda *et al*, 2001, 2002; del Bano *et al*, 2003). In this study, we investigated the inhibitory effect of CA on TNF-α-induced HASMCs migration and MMP-9 activity.

3.2 Materials and Methods

3.2.1 Materials

3.2.1.1 Instruments

CO_2 incubator	NUAIRE, MN, USA
Laminar flow	NUAIRE, MN, USA
Microscope	Nikon, Japan
pH meter	HANNA, RI, USA
Stirrer/Hotplate	Corning, Taiwan
Waterbath tank	TKS, Taiwan
Haemocytometer	Boeco, Germany
Eppendorf centrifugator	Hamburg, Germany
Pipetman	Gilson, France
Spectrophotometer	HITACHI, Japan
Spectrophotometer	Beckman Coulter, CA, USA
MicroPlate fluorescence reader	Bio-Tek, VT, USA
Shaking incubator	Orbital, VA, USA
ELISA plate reader	Bio-Tek, VT, USA
Electrophoresis tank	Bio-Rad, CA, USA
Transfer system	Bio-Rad, CA, USA

Electrophoresis chamber   Bio-Rad, CA, USA

Power supply   Hoefer, CA, USA

3.2.1.2 Chemicals

40 % Acrylamide   Amresco, OH, USA

2, 7-dichlorofluorescein diacetate (DCFH-DA)   Molecular Probe, OR, USA

3-(4, 5-dimethylthiazol-2-yl)-2, 5-diphenyl tetrazolium bromide (MTT)

                                             Sigma, MO, USA

Acetic acid   Amresco, OH, USA

Bovine serum albumin (BSA)   Sigma, MO, USA

Bradford   Bio-Rad, CA, USA

CA   Sigma, MO, USA

Chloroform   BDH, Poole, England

Diethyl pyrocarbonate (DEPC)   Sigma, MO, USA

Dimethyl sulfoxide (DMSO)   Amresco, OH, USA

Dodecylsulfate sodium salt (SDS)   Amresco, OH, USA

Enhanced chemiluminescence (ECL)   Upstate, CA, USA

Ethanol   景明化工, Taichung, Taiwan

F12K   Sigma, MO, USA

Fetal bovine serum (FBS)   Gibco, NY, USA

Gelatin   Amresco, OH, USA

Glycerol   Amresco, OH,USA

Glycine   Amresco, OH, USA

Hepes	Gibco, NY, USA
Invasion assay kit	Chemicon, CA, USA
Isopropanol	Sigma, MO, USA
Methanol	Tedia, OH, USA
Nuclear extract kit	TransAM, CA, USA
NF-κB kit	TransAM, CA, USA
Penicillin-Streptomycin	Gibco, NY, USA
Recombinant human TNF-α	Cytolab, Rehovot, Israel
Sodium biocarbonate	Sigma, MO, USA
Sodium chloride	Sigma, MO, USA
Temed	Amresco, OH, USA
Tris base	Amresco, OH, USA
Tris-HCl	Amresco, OH, USA
Triton X-100	Amresco, OH, USA
Trizol	Invitrogen, CA, USA
Trypsin	Sigma, MO, USA
Trypan blue	Sigma, MO, USA
Tween-20	Amresco, OH, USA

3.2.1.3 Antibodies

Primary antibodies

Mouse anti-human β-actin	Abcam, Cambridge, UK
Rabbit anti-human matrix metallproteinases-9	Abcam, Cambridge, UK

Secondary antibodies

Sheep anti-mouse IgG antibody   Abcam, Cambridge, UK

Goat anti-rabbit IgG antibody   Abcam, Cambridge, UK

3.3 Methods

3.3.1 DPPH scavenging assay

Free radical scavenging effect was determined using the free radical generator DPPH (2, 2-diphenyl-1-picrylhydrazyl) by a similar method to Yamaguchi *et al*, 1998. Briefly, the reaction mixture contained 500 μl of CA concentrations (0-200 μmol/l) and 500 μl of DPPH (0.5 mmol/l in methanolic solution). The DPPH radical scavenging activity was evaluated by measuring the decrease of DPPH radical detected at 517 nm and by determining the difference in the peak area between control and reaction mixture. Inhibition % was calculated via Eq.

$$\text{Inhibition \%} = (B1\text{-}B0/B0) \times 100$$

(where B0: is the absorbance of control. B1: is the absorbance of reaction mixture.)

The decoloration was plotted against the sample extract concentration in order to calculate the IC_{50} values (inhibitory concentration 50 μmol/l), which is the amount of sample necessary to decrease the absorbance of DPPH by 50 %.

3.3.2 Trolox equivalent antioxidant capacity (TEAC) assay

The assay was carried out using a spectrophotometer by the improved $ABTS^{\bullet+}$ method as described by Re *et al*, 1999 with slight modification. Briefly, $ABTS^{\bullet+}$ radical cation

was generated by a reaction of 7 mmol/l 2,2'-azinobis(3-ethyl-benzothiazoline-6-sulfonicacid-diammoniumsalt) (ABTS) and 2.45 mmol/l potassium persulfate. The reaction mixture was allowed to stand in the dark for 16 h at room temperature and used within 2 days. The ABTS$^{\bullet+}$ solution was diluted with ethanol to an absorbance of 0.700±0.050 at 734 nm. All samples were diluted appropriately to provide 20-80 % inhibition of control absorbance. Fifty microliters of the diluted sample were mixed with 1.9 ml of diluted ABTS$^{\bullet+}$ solution. The assay with the mixture was carried out in triplicate, the mixture was allowed to stand for 6 min at room temperature and the absorbance was immediately recorded at 734 nm (Li *et al*, 2007). Trolox solution (final concentration 0~15 μmol/l) was used as a reference standard. The results were expressed as μmol/l Trolox of CA.

3.3.3   Isolation of low density lipoproteins

Blood was collected from healthy donors after a 12 h overnight fasting using EDTA as anticoagulant. Plasma was obtained after low-speed centrifugation of the blood, adjusted to a density of 1.21 g/ml with KBr and a discontinuous density gradient was made by overlaying the plasma solution with a 10 mmol/l PBS and 1 mmol/l EDTA pH 7.4. LDL were isolated after ultracentrifugation as described previously (Vieira *et al*, 1996). The LDL fraction was exhaustively dialyzed against PBS buffer pH 7.4 without EDTA in the dark, filtered through a 0.45 μm filter, stored at 4 °C under nitrogen and used in 24-72 h.

3.3.4   Inhibition of LDL Oxidation

LDL were oxidised using the classical copper-induced LDL auto-oxidation. Incubations were carried out at 37 °C for measuring the diene conjugated formation (Vieira *et al*, 1996). Increasing concentrations of CA (0~10 μmol/l) dissolved in DMSO were present in the incubation media. Briefly, 0.9 mg/ml of LDL total cholesterol was incubated in PBS in the presence of $CuSO_4$ (50 μmol/l). After incubation, 150 μL EDTA (2 mmol/l) was added. A 100 μL portion of the mixture was then transferred to vials containin 0.9 ml of 2-propanol. The precipitates were removed by centrifugation. The concentration of conjugated diene in the supernatant was determined by absorption at 234 nm.

3.3.5 Cell culture

HASMCs were purchased from Food Industry Research and Development Institute, 新竹, Taiwan. (CCRC 60293). They were maintained in Ham's F12K containing 10 % fetal bovine serum, 2 mmol/l L-glutamine, 1.5 g/l sodium bicarbonate, 10 mmol/l HEPES, 10 mmol/l TES, 0.05 mg/ml ascorbic acid, 0.01 mg/ml transferrin, 0.01 mg/ml insulin, 10 ng/ml sodium selenite, 0.03 mg/ml ECGs. All experiments were performed with HASMCs from passages 21 to 31, which were grown to 80-90 % confluence and made quiescent by serum starvation (0.1 % FBS) for at least 24 hours.

3.3.6 Cell viability assay (MTT assay)

The cytotoxic effect of CA on HASMCs was investigated using 3-(4, 5-dimethylthiazol-2-yl)-2, 5-diphenyl tetrazolium bromide (MTT) assay (Chen *et al*,

2002). The principle of this assay is that mitochondria dehydrogenase in viable cells reduces MTT to a blue formazan. Briefly, the cells were grown in 96-well culture plates at a density of 1×10^4 cells per well in F-12K culture medium and incubated with various concentrations of CA for 24 hours. 10 μl MTT (5 mg/ml) were then added to each well and incubation continued at 37 °C for an additional 4 hours. The medium was then carefully removed, so as not to disturb the formazan crystals which had formed. Dimethyl sulphoxide (100 μl), which solubilizes formazan crystals, was added to each well and absorbance of the solubilized blue formazan was measure the optical density at 590 nm using μQuant Microplate Spectrophotometer (Bio-Tek, VT, USA). All determinations were performed according to three individual experiments. The data were shown mean±SD as percentage of control.

3.3.7 Gelatin zymography for MMP-9

MMP-9 activity in conditioned medium of cultured HASMCs was analyzed by substrate-gel electrophoresis (zymography) using SDS-PAGE (10 %) containing 0.1 % gelatin. Substrate gel zymography of the activity of MMP-9 was performed with a Mini-Protein II apparatus from Bio-Rad, according to a method described previously (Demeule *et al*, 2000). Cells were grown to sub-confluence and were rinsed with phosphate-buffered saline (PBS) and then incubated in serum-free medium for 24 h. Equal volumes of samples of conditioned cell culture medium were mixed with sample buffer containing 62.5 mmol/l Tris-HCl (pH 6.8), 10 % glycerol, 2 % SDS, and 0.00625 % (w/v) bromophenol blue, loaded onto the gel and separated by electrophoresis. Thereafter, gels were washed 3 times for 30 minutes at room

temperature in buffer (50 mmol/l Tris-HCl, pH 8.0, 5 mmol/l $CaCl_2$, 0.02 % NaN_3, and 2.5 % Triton X-100) and incubated for 18 h at 37 °C with the same buffer except Triton X-100. Gels were stained with Coomasssie Brillant Blue R-2500 (0.1 %) and destained in 5 % methanol and 7 % acetic acid. Gelatinolytic activity appeared as a clear band on a blue background.

3.3.8   Bradford protein assay

The Bradford assay (Bradford**,** 1976), a colorimetric protein assay, is based on an absorbance shift in the dye Coomassie when bound to arginine and hydrophobic amino acid residues present in protein. The anionic (bound) form of the dye is blue and has an absorption spectrum maximum historically held to be at 595 nm. The cationic (unbound) forms are green and red. The increase of absorbance at 595 nm is proportional to the amount of bound dye, and thus to the amount (concentration) of protein present in the sample. Standard solutions contain a range of 0 to 25 micrograms protein (BSA) in 800 μl H_2O, followed by adding 200 μl dye reagent and incubate 5 min. l μl of sample solution add into 799 μl H_2O, followed by adding 200 μl dye reagent and incubated for 5 min. The absorbance was read at 595 nm. The results for made a standard curve and the protein concentration of sample was determined by standard curve.

3.3.9   Western blot analysis

HASMCs were treated with various concentrations of CA in the presence of 100

ng/ml TNF-α. Cellular lysates were prepared in a lysis buffer containing 10 mmol/l Tris/HCl (pH 8), 0.32 mol/l sucrose, 5 mmol/l Ethyienediamine Teraacetate Disodium Salt (EDTA), 1 % Triton X-100, 2 mmol/l 1, 4-Dithio-D,L-thereitol (DTT), 1 mmol/l PMSF. The cells were disrupted and extracted at 4 °C for 30 min. After centrifugation at 13,000 rpm for 15 min, the supernatant was obtained as the cell lysate. Protein concentrations were measured using the bradford assay. Total protein (20 μg) were subjected to SDS-PAGE (10 %) and blotted on PVDF membranes (Shishodia *et al*, 2003). Nonspecific binding was blocked by soaking the membrane in PBS-Tween 20 (PBST) buffer containing 50 g/l nonfat milk. The membrane was incubated with monoclonal mouse anti-human β-actin (1:1000) and polyclonal rabbit anti-human MMP-9 (1:1000). Subsequently, the membrane was incubated with sheep anti-mouse IgG antibody (1:5000) and goat anti-rabbit IgG antibody (1:5000). The protein levels were determined using the enhanced chemiluminescence detection reagents (Upstate, CA, USA) and high performance chemiluminescence film (Amersham, IL, USA). Incubation with mouse anti-human β-actin antibody was also performed as an internal control. Results were quantified with scanning densitometer using an image analysis system with software.

3.3.10 Preparation of nuclear extract

Nuclear protein extracts of HASMCs were prepared using a nuclear extract kit (TransAM nuclear extract kit, CA, USA). Cells were lysed in hypotonic buffer and centrifuge suspension for 30 sec at 14000×g in a microcentrifuge pre-cooled at 4 °C (Dschietzig *et al*, 2001). Then resuspend nuclear pellet in 50 μl complete lysis buffer

containing 10 mmol/l DTT, lysis buffer AM2, and protease inhibitor cocktail by pipetting up and down. The suspension was incubates for 30 min on ice, and centrifuged for 10 min at 14,000×g in a microcentrifuge pre-cooled at 4 °C. Transfer supernatant and stored at -80 °C. Protein concentrations were measured using the bradford protein assay.

3.3.11   ELISA-Based Nuclear Factor-κB Assay

Additionally to gel-shift assays, an ELISA-based kit was used for quantitative detection of NF-κB activity (TransAM NF-κB kit, CA, USA). For each sample, 20 μl of nuclear extracts (5 μg protein) were used according to the instructions of the manufacturer (Yu *et al*, 2007). Nuclear extracts were incubated with the oligonucleotide-coated wells for 60 min. Where indicated a competitor for NF-κB binding (NF-κB wild-type consensus oligonucleotide) was added in molar excess prior to the probe. The wells were then washed and incubated with the primary antibodies for p50 and p65 for 60 min. After incubation with a horseradish peroxidase-conjugated secondary antibody, a substrate was added to produce blue colour and then for quantitation by μQuant Microplate Spectrophotometer (Bio-tek, VT, USA). The absorbance was read at 590 nm and the blank were subtracted from all measurements.

3.3.12   Cell migration assay

VSMCs invasion through the extracellular matrix was determined by using a commercial cell invasion assay kit (Chemicon, CA, USA). HASMCs (1.5×10^5

cells/300 μl) were resuspended in conditioned medium collected from pretreatment with CA and TNF-α-treated cells for 23 h, and added to the upper components of migration chamber (Bedoui *et al*, 2005). Five hundred microliters of same conditioned medium were added to the lower compartment of migration chamber. Cells without TNF-α-treated conditioned medium served as control. The migration chambers were incubated at 37 °C for 24 h in 5 % CO_2. After incubation, the inserts were removed from the wells, and the cells on the upper side of the filter were removed using cotton swabs. The filters were fixed, and stained according to the manufacturer's instructions. The cells that invaded and were located on the underside of the inserts. Then transfer 100 μl of the dye mixture to a 96-well plate, and measure the optical density at 560 nm.
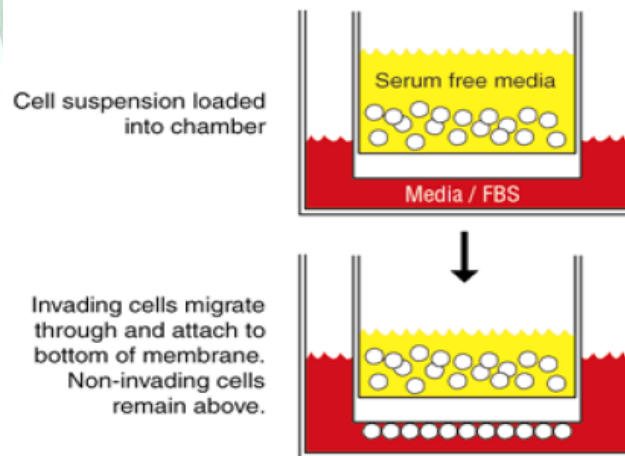
3.3.13 Measurement of intracellular ROS

HASMCs were pretreated with 10 and 20 μmol/l CA for 1 hour and induced by

TNF-α (100 ng/ml) for 23 h. Then were incubated with 10 μmol/l 2,7-dichlorofluorescein (DCF) diacetate (DCFH-DA) for 30 min, which is converted to DCF by intracellular esterase (Kim *et al*, 2006). The latter was then oxidized by ROS to the highly fluorescent DCF. The fluorescence of each dish was immediately analyzed at excitation wavelength of 485 nm and emission wavelength of 528 nm by FLx800 microplate fluorescence reader (Bio-tek, VT, USA). All measurements were at least triplicated.

3.3.14 Statistical analysis

Results are shown as mean±SD. Statistical analyses of MTT were performed using One-way ANOVA followed by Dunnett's test and others were performed using One-way ANOVA followed by Duncan's Multiple Range Test. A value of $p < 0.05$ was considered statistically significant.

3.4　Results

3.4.1　The antioxidant activity of CA

Free radical scavenging effect was determined using the free radical generator DPPH (2, 2-diphenyl-1-picrylhydrazyl) and the IC_{50} of DPPH assay is 35.92±1.65 μmol/l (Table 3-1). In inhibition of LDL oxidation assay, LDL was oxidatied using the classical copper-induced LDL auto-oxidation and the IC_{50} of inhibition of LDL oxidation is 5.63±0.19 μmol/l (Table 3-1). The TEAC assay is based on the reduction of the ABTS (2, 2′-azino-bis-(3-ethylbenzthiazoline-6-sulfonic acid)) radical cation by antioxidants and TEAC value of CA is 5.75±0.49 μmol/l (Table 3-1). A value of 1 TEAC in a sample is defined as a concentration equivalent to 1 μmol/l Trolox, a water-soluble analog of α-tocopherol.

3.4.2　Cytotoxicity of CA on HASMCs.

The cytotoxity of CA on HASMCs were evaluated using MTT assay. The HASMCs (1×10^4 cells/well) were incubated for 24 hours in cultures in 96-well with various concentrations of CA (0, 10, 20, 30, 50, and 75 μmol/l). Dose-dependent cytotoxic effect of CA against HASMCs was shown in Fig. 3-1 (100 %, 94.9±1.2 %, 92±0.5 %, 84.9±0.6 %, 79.7±1.6 %, and 67.7±2.6 %, respectively.). According to the MTT assay, we chose 10 and 20 μmol/l of CA to do all the following experiments.

3.4.3 CA prevents TNF-α-induced activation of MMP-9 in HASMCs.

The inhibitory effect of CA on TNF-α-induced MMP-9 activation were analysed by gelatin zymography. HASMCs were pretreated with 10 and 20 μmol/l CA for 1 h, and then induced by TNF-α (100 ng/ml) for additional 23 h. As shown in Fig. 3-2, MMP-9 secretion was markedly induced by TNF-α, and suppressed by CA. The 20 μmol/l CA treatment is more effective on activation of MMP-9 than 10 μmol/l CA.

3.4.4 CA suppresses TNF-α-induced MMP-9 expression in HASMCs.

The effect of MMP-9 expression by CA in VSMCs was assessed by Western blot. HASMCs were pretreated with 10 and 20 μmol/l CA for 1 h, and induced by TNF-α (100 ng/ml) for 23 h. MMP-9 expression was markedly induced by TNF-α, and suppressed by CA (Fig. 3-3).

3.4.5 CA suppresses nuclear translocation of NF-κB p50 and p65 in TNF-α-induced HASMCs.

To determine whether the inhibitory effect of CA on the TNF-α-induced expression of MMP-9 is medicated via NF-κB, we measured the nuclear translocation of p50 and p65 of the NF-κB family. Treatment of TNF-α (100 ng/ml) for 23 h enhanced the nuclear translocation of p50 (Fig. 3-4) and p65 (Fig. 3-5). Pretreatment

of HASMCs with 10 and 20 μmol/l CA prior to TNF-α stimulation did significantly prevent the nuclear translocation of p50 and p65. As shown in Fig. 3-4, the 20 μmol/l CA treatment is more effective on decreased nuclear translocation of NF-κB p50 than 10 μmol/l CA. In Fig. 3-5, the 20 μmol/l CA treatment is more effective on decreased nuclear translocation of NF-κB p65 than 10 μmol/l CA.

3.4.6 CA suppresses TNF-α-induced HASMCs migration.

HASMCs (1.5×10^5 cells/300 μl) were resuspended in pretreated with 10 and 20 μmol/l CA for 1 h, and induced by TNF-α (100 ng/ml) for 23 h. As shown in Fig. 3-6, the migration of HASMCs was increased by treatment with TNF-α when compared with TNF-α-untreated control cells. The stimulatory effect of TNF-α was significantly reduced by CA. The 20 μmol/l CA treatment is more effective on decreased HASMCs migration than 10 μmol/l CA.

3.4.7 CA suppresses TNF-α-induced ROS generation.

To characterize the events underlying TNF-α-induced migration, we examined the generation of ROS after TNF-α treatment in HASMCs. HASMCs were exposed to TNF-α (100 ng/ml) for 23 h, and DCF fluorescence produced was measured (Fig. 3-7). The production of ROS was induced by TNF-α and decreased by CA. The 20 μmol/l CA treatment is more effective on reduced ROS generation than 10 μmol/l CA.

3.5 Discussion

In this study, we investigated the effect of CA on HASMCs migration and MMP-9 activation induced by TNF-α. CA lowered the secretion and protein expression of MMP-9 by gelatin zymography and Western blot assays. It also decreased nuclear translocation of nuclear factor-κB (NF-κB) p50 and p65. In addition, the migration assay showed that CA effectively inhibited the TNF-α-induced migration of HASMCs as compared with the control group. In our *in vitro* study, we also found that CA could scavenge DPPH (2, 2-diphenyl-1-picrylhydrazyl) radicals, alkoxyl radical (RO•), and peroxyl radical (ROO•). It is approximately 5-6-folds more potent than Trolox in antioxidative ability. It also could suppress TNF-α-induced intracellular ROS production.

Sage (*Salvia officinalis*) and rosemary (*Rosmarinus officinalis*) are popular Labiatae herbs used as spices and folk medicines around the world (Masuda *et al*, 2002). In the 1950s, it was reported that an extract of rosemary leaves contained high antioxidative activity (Huang *et al*, 2005). In addition, sage and rosemary extracts contained 0.29 % and 0.1-0.5 % CA, respectively (Huang *et al*, 1994; Kiyofumi *et al*, 2004). In the present study, we found that 20 μmol/l of CA did not have any significant effect on the cytotoxity of HASMCs from MTT test (Fig. 3-1). Therefore, we chose 10 and 20 μmol/l of CA to do all the experiments.

The migration of SMCs from the tunica media to the subendothelial region is a key event in the development and progression of many vascular diseases including atherosclerosis and post-angioplasty restenosis (Maeda *et al*, 2002). MMPs (MMP-2

and MMP-9) activities may contribute to the pathogenesis of atherosclerosis by facilitating migration of VSMCs (Jones *et al*, 2003). Although MMP-2 and MMP-9 have similar substrate specificities, the regulation of their expression are different. MMP-2 is constitutively expressed by several cell types, including SMCs, and its expression is not induced by cytokines or growth factors. In contrast, the basal levels of MMP-9 are usually low, and its expression can be induced by treatment of cells with TNF-α, but not platelet-derived growth factor (PDGF) or thrombin (Cho *et al*, 2000; Galis *et al*, 1994). Therefore, we have investigated the effect of CA on the migration of HASMCs and activation of MMP-9. The results indicated that the migration of HASMCs was significantly induced by TNF-α, and suppressed by CA (Fig. 3-6). This inhibition against TNF-α-induced migration of HASMCs is consistent with the inhibition of activation and expression of MMP-9 (Fig. 3-2 and Fig. 3-3). A similar result was seen when HASMCs were pretreated with other polyphenolic compound, such as tea flavonoid epigallocatechin-3-gallate (20 μmol/l), quercetin (40 μmol/l), and other flavonoids (Kim et al., 2005; Moon et al., 2003).

The NF-κB family controls the expression of genes involved in the inflammation and immune response (Baeuerle, 1991). In the cytoplasm, inactive NF-κB exists as a heterodimeric complex of subunits p50 and p65 that binds to a cytoplasmic protein, IκB (Baeuerle and Henkel, 1994). Upon activation, IκB is rapidly degraded, and the p50/p65 heterodimer is translocated from the cytoplasm into the nucleus where the dimmer interacts with regulatory κB elements in promoters and enhancers, thereby controlling gene transcription (Baeuerle and Baltimore, 1988). NF-κB is activated by a multitude of stimuli, including various inflammatory cytokines and reactive oxygen intermediates (Baeuerle and Baltimore, 1998; Grilli *et*

al, 1993; Muller *et al*, 1997), which are activated in atherosclerotic lesions (Brand *et al*, 1996). In the present study, CA reduced cytokine-induced nuclear translocation of p50 (Fig. 3-4) and p65 (Fig. 3-5) in HASMCs.

Much further work, which is beyond the scope of the present study, is necessary to elucidate the mechanisms underlying the synergistic regulation of MMP secretion by cytokines. We focused instead on defining the role played by the NF-κB transcription factor in the regulation of MMPs in HASMCs. A functional NF-κB site occurs in the proximal stimulatory region of the MMP-9 promoter (Sato and Seiki, 1993; Fini *et al*, 1994) and deletion of this site reduces upregulation of reporter gene constructs in response to cytokines. Until now, however it has been unclear what contribution NF-κB plays in the upregulation of the endogenous MMP-9 gene. Previous study has demonstrated that transient overexpression of IκBα in vascular SMCs only partially impaired upregulation of MMP-9, suggesting that NF-κB simply plays a permissive role in the upregulation of MMP-9 (Bond *et al*, 2001). In the present study, CA reduced cytokine-induced expression of MMP-9 and prevented the nuclear translocation of p50 (Fig. 3-4) and p65 (Fig. 3-5) in HASMCs. We suggested that inhibitory mechanisms of CA might interrupt a signaling cascade involving MMP-9 transcription-mediated activation of NF-κB.

Several studies have indicated that ROS are implicated in the activation of NF-κB (Muller *et al*, 1997). The current study shows that the ROS production stimulated by TNF-α was decreased by CA pretreatment in HASMCs (Fig. 3-7). Based on this result, we proposed that the inhibitory effect of CA on MMP-9 expression and NF-κB activation may be due to its antioxidant and anti-inflammatory properties. In our *in vitro* study, we also found that CA could scavenge DPPH (2,

2-diphenyl-1-picrylhydrazyl) radicals, alkoxyl radical (RO$^{\bullet}$), and peroxyl radical (ROO$^{\bullet}$) (Table 3-1). It is approximately 5-6-folds more potent than Trolox in antioxidative ability (Table 3-1). Since atherosclerosis is a chronic inflammatory disease associated with increased oxidative stress in the VSMCs, it would be conceivable that the anti-atherogenic effects of CA might due to its antioxidative and anti-inflammatory properties. The inhibition of cytokine-induced MMP-9 expression has been described for other substances with anti-inflammatory properties such as tea flavonoid epigallocatechin-3-gallate, quercetin, and other flavonoids (Kim *et al*, 2005; Moon *et al*, 2003).

3.6 Conclusion

In this study, CA effectively inhibited the TNF-α-induced migration of HASMCs as compared with the control group. The ROS production, MMP-9 secretion and expression, nuclear translocation of NF-κB p50 and p65 were reduced by CA pretreatment. These results led us to conclude that CA could restrict the migration ability of HASMCs by suppressing MMP-9 through down-regulation of NF-κB.

Table 3-1. Antioxidative capacities of CA *in vitro*.

	Inhibition of LDL Oxidation (IC_{50}, µmol/l)	DPPH radicals scavenging ability (IC_{50}, µmol/l)	Trolox Equivalent Antioxidant Capacity (TEAC) assay
Carnosic acid	5.63±0.19	35.9±1.7	5.75±0.49

All values are mean±SD. IC_{50} values were obtained from the concentration response curves; n =3.
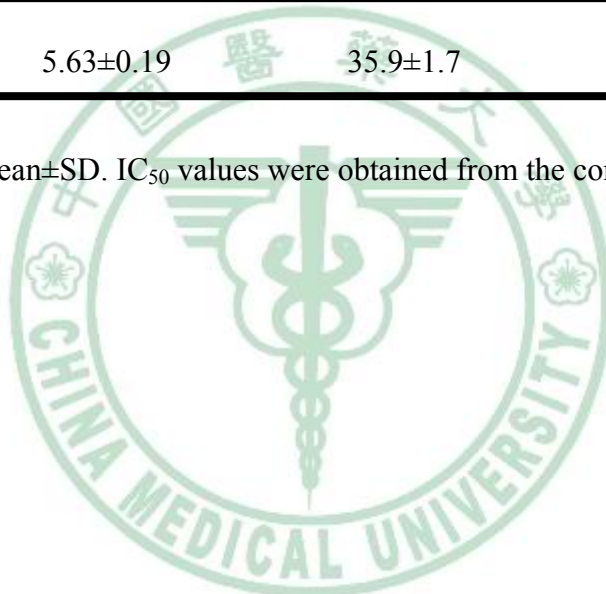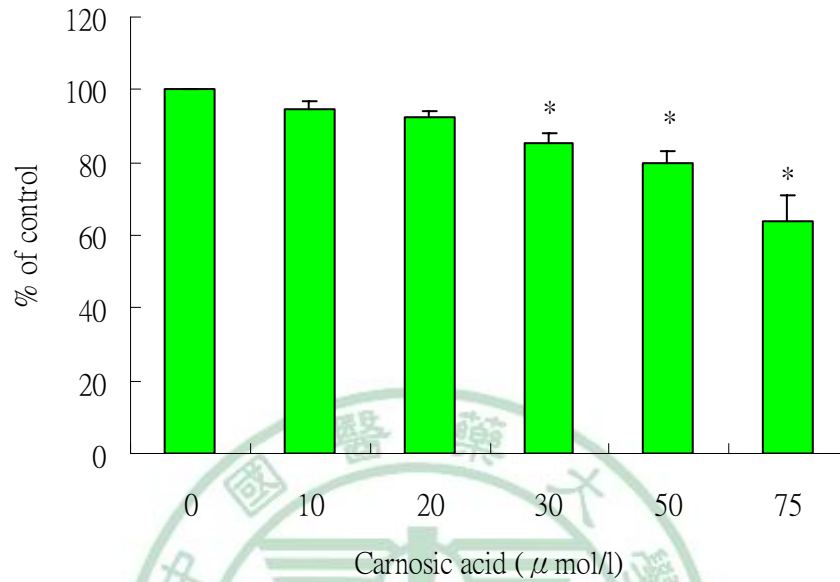
Fig. 3-1. Cytotoxic effect of carnosic acid (CA) on human aortic smooth muscle cells (HASMCs) with MTT test. HASMCs were treated with increasing concentrations (10~75 μmol/l) of CA for 24 h in 10 % FBS-F12K. Statistical analyses of MTT were performed using One-way ANOVA followed by Dunnett's test; n=3. *$p<0.05$ compared with control.
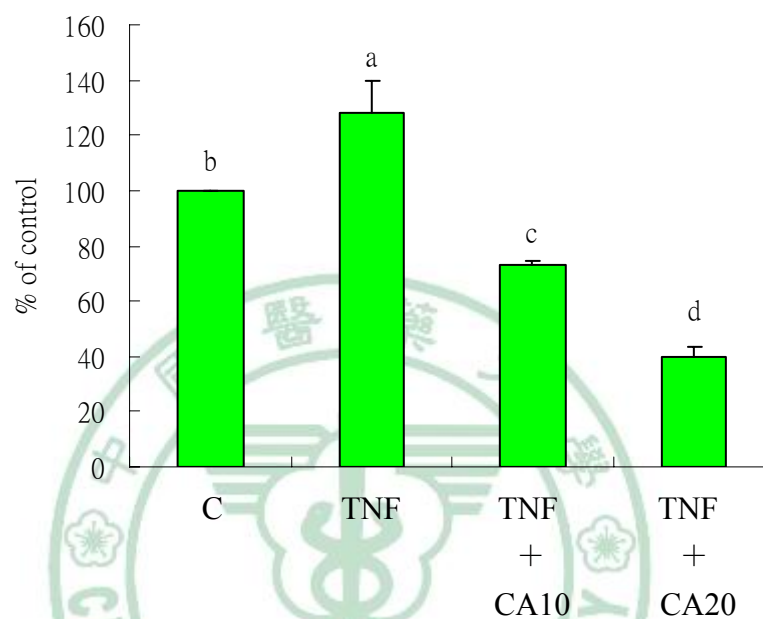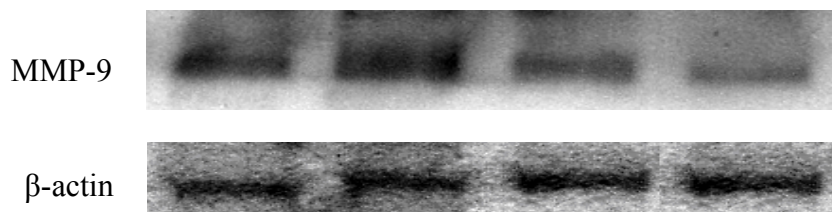
(A)

MMP-9

(B)

Fig. 3-2. Effect of carnosic acid (CA) on the MMP-9 activity of TNF-α-induced human aortic smooth muscle cells (HASMCs). HASMCs were pretreated with 10 and 20 μmol/l CA for 1 h, and induced by TNF-α (100 ng/ml) for additional 23 h. The activation of MMP-9 was assessed by gelatin zymography (A). Densitometric analysis was conducted with image analysis system software to quantify gelatin zymography data (B). Values are mean±SD, n=3. [a-d]Means with different letters are significantly different compared at $p<0.05$. Abbreviation: C (control without TNF-α or CA), TNF (TNF-α), CA10 (CA 10 μmol/l), CA20 (CA 20 μmol/l).
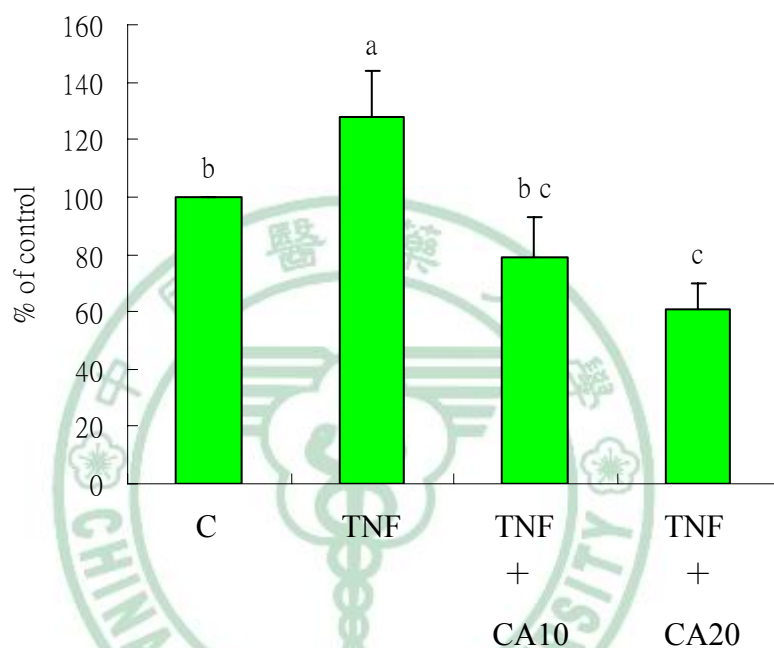
(A)

MMP-9

β-actin

(B)

Fig. 3-3. Carnosic acid (CA) inhibits the protein expression of MMP-9 in human aortic smooth muscle cells (HASMCs). HASMCs were pretreated with 10 and 20 μmol/l CA for 1 h, and induced by TNF-α (100 ng/ml) for additional 23 h. The expression of MMP-9 was assessed by western blot analysis. Representative western blot showing MMP-9 protein levels in cell lysates (top) and β-actin (bottom) (A). Densitometric analysis was conducted with image analysis system software to quantify western blot data (B). Values are mean±SD, n=3. [a-c]Means with different letters are significantly different compared at $p<0.05$. Abbreviation: C (control without TNF-α or CA), TNF (TNF-α), CA10 (CA 10 μmol/l), CA20 (CA 20 μmol/l).

Fig. 3-4. Effect of carnosic acid (CA) on TNF-α-induced activation of NF-κB p50 in human aortic smooth muscle cells (HASMCs). HASMCs were pretreated with 10 and 20 μmol/l CA for 1 h and induced by TNF-α (100 ng/ml) for 23 h. Nuclear extracts were prepared and analyzed for activation of NF-κB family. Five micrograms of nuclear protein was used in each experiment. Values are mean±SD, n=3. [a-d]Means with different letters are significantly different compared at $p<0.05$. Abbreviation: C (control without TNF-α or CA), TNF (TNF-α), CA10 (CA 10 μmol/l), CA20 (CA 20 μmol/l).
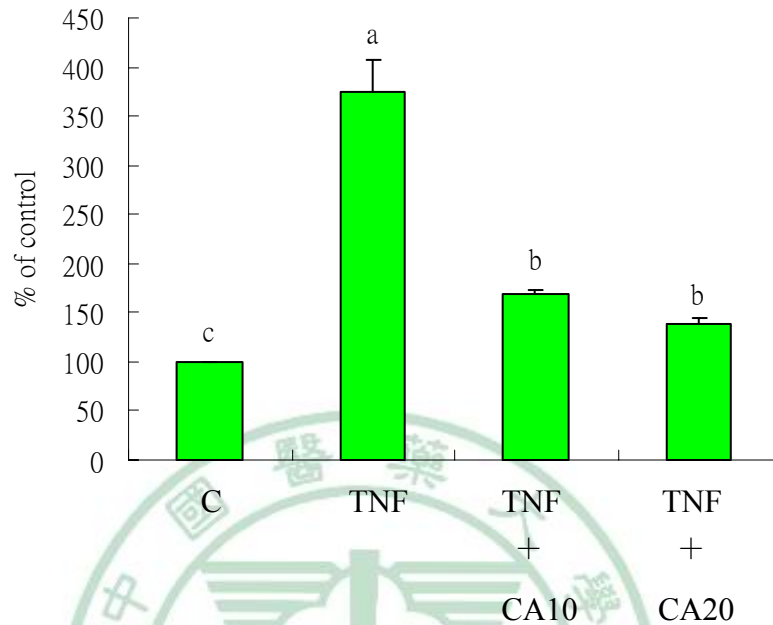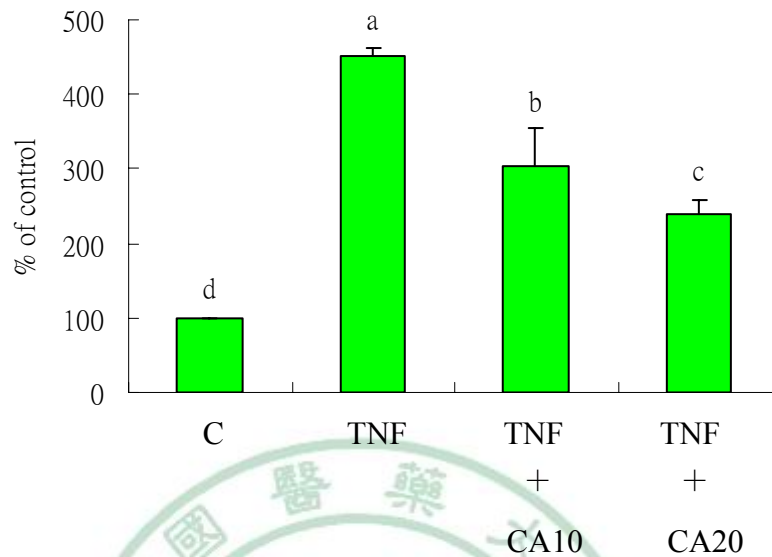
Fig. 3-5. Effect of carnosic acid (CA) on TNF-α-induced activation of NF-κB p65 in human aortic smooth muscle cells (HASMCs). HASMCs were pretreated with 10 and 20 μmol/l CA for 1 h and induced by TNF-α (100 ng/ml) for 23 h. Nuclear extracts were prepared and analyzed for activation of NF-κB family. Five micrograms of nuclear protein was used in each experiment. Values are mean±SD, n=3. [a-d]Means with different letters are significantly different compared at $p<0.05$. Abbreviation: C (control without TNF-α or CA), TNF (TNF-α), CA10 (CA 10 μmol/l), CA20 (CA 20 μmol/l).
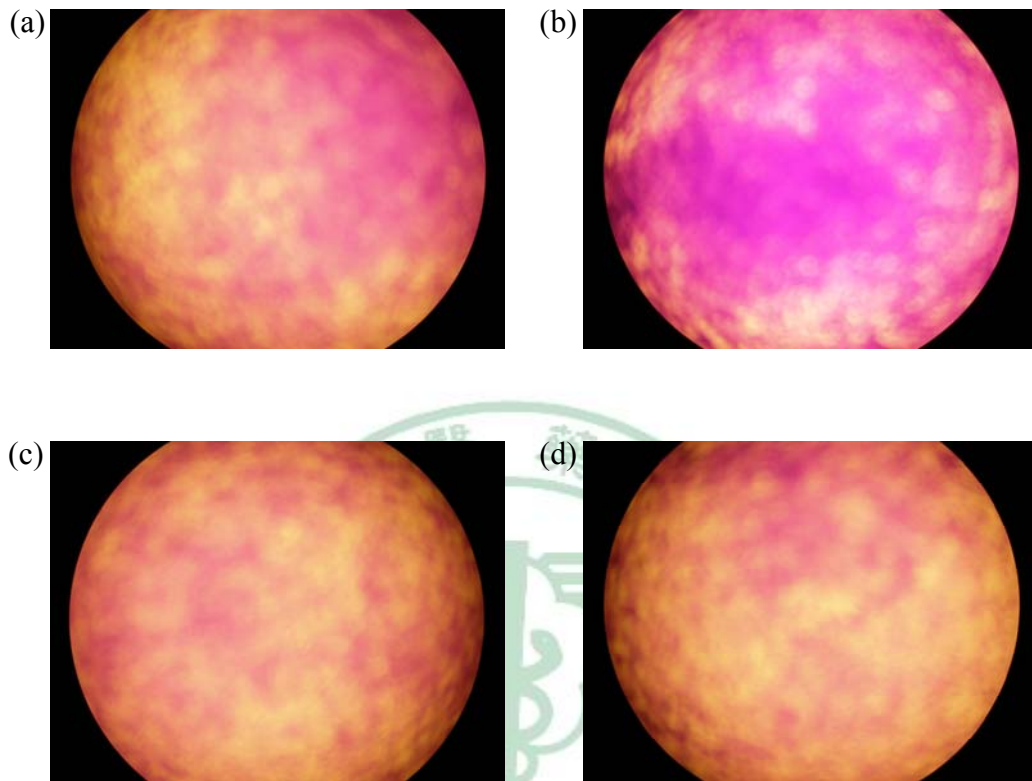
(A)

(a)

(b)

(c)

(d)

(B)
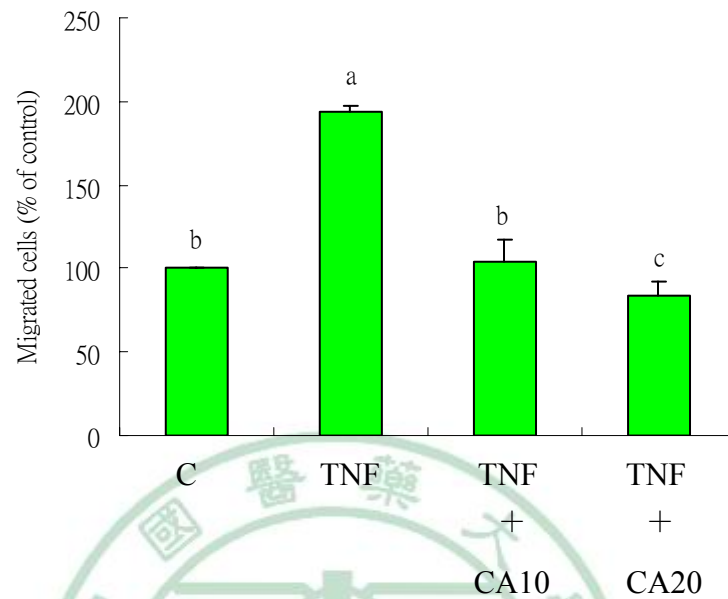
Fig. 3-6. Effect of carnosic acid (CA) on migrarion of human aortic smooth muscle cells (HASMCs) induced by TNF-α treatment. (A) Microphotograph of migrated cells without TNF-α or CA (a), with TNF-α (100 ng/ml) (b), with TNF-α (100 ng/ml) and 10 μmol/l of CA (c), and with TNF-α (100 ng/ml) and 20 μmol/l of CA (d) were captured. (B) HASMCs (1.5×10^5 cells/300 μl) were resuspended in conditioned medium collected from TNF-α treated cells for 23 h, and added to the upper components of migration chamber in the presence of 10 and 20 μmol/l CA. Values are mean±SD, n=3. [a-c]Means with different letters are significantly different compared at *p*<0.05. Abbreviation: C (control without TNF-α or CA), TNF (TNF-α), CA10 (CA 10 μmol/l), CA20 (CA 20 μmol/l).

(A)

(a)

(b)

(c)

(d)
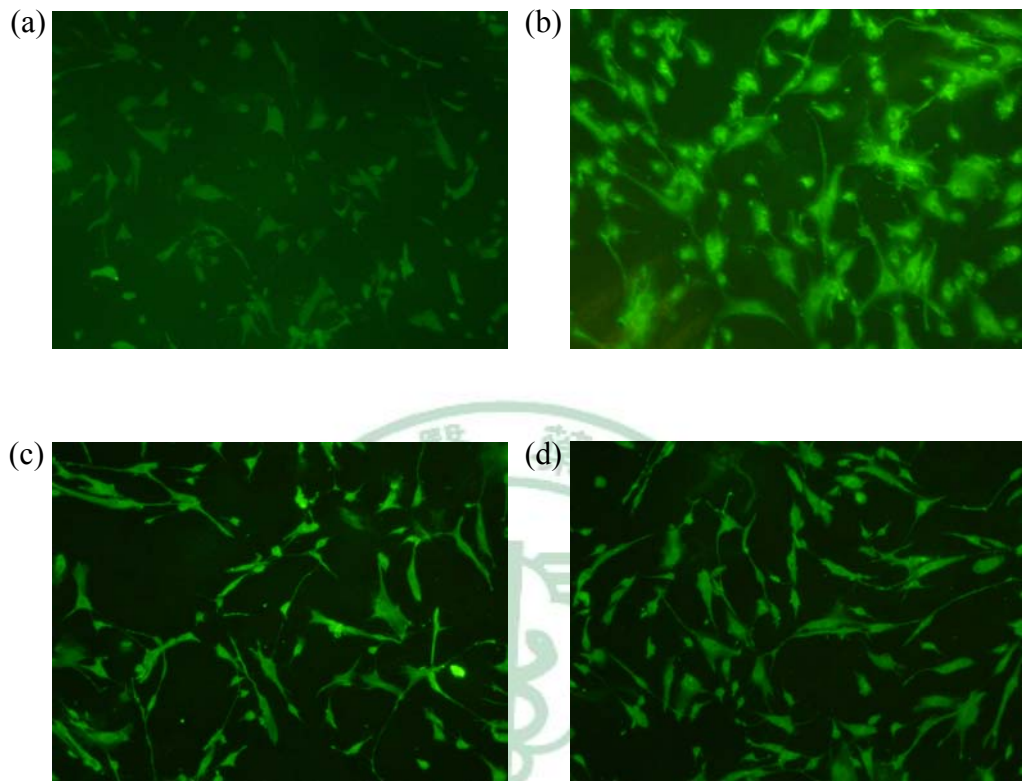
(B)
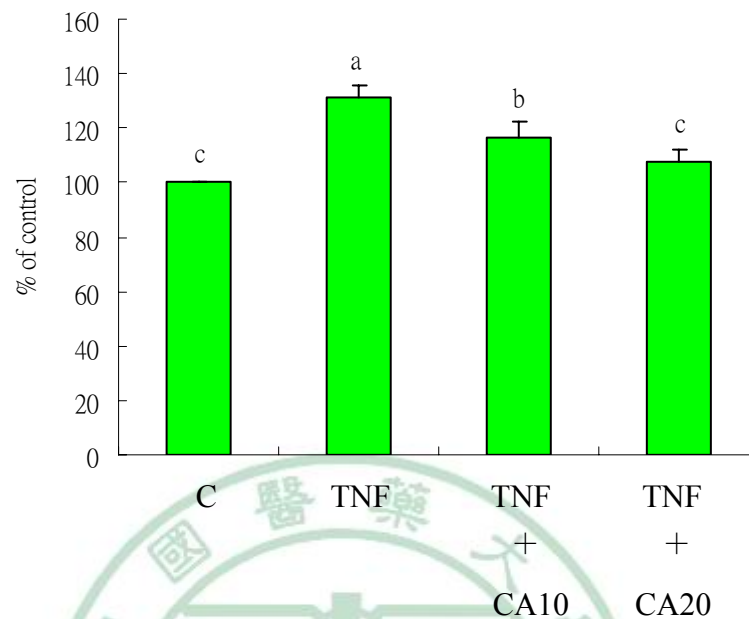
Fig. 3-7. Effect of carnosic acid (CA) on TNF-α-induced ROS production in human aortic smooth muscle cells (HASMCs). (A) Microphotograph of ROS production in HASMCs without TNF-α or CA (a), with TNF-α (100 ng/ml) (b), with TNF-α (100 ng/ml) and 10 μmol/l of CA (c), and with TNF-α (100 ng/ml) and 20 μmol/l of CA (d) were captured. (B) HASMCs were pretreated with 10 and 20 μmol/l CA for 1 h and induced by TNF-α (100 ng/ml) for 23 h. Values are mean±SD, n=3. [a-c]Means with different letters are significantly different compared at $p<0.05$. Abbreviation: C (control without TNF-α or CA), TNF (TNF-α), CA10 (CA 10 μmol/l), CA20 (CA 20 μmol/l).

Chapter 4

Summary

Curcumin is a polyphenol derived from the plant *Curcuma longa*. Carnosic acid (CA) is the primary phenolic compound in rosemary. In this study, we investiguate the effect of curcumin and CA on human aortic smooth muscle cells (HASMCs) migration and MMP-9 activation induced by TNF-α. The results indicated that curcumin and CA lowered the secretion and protein expression of MMP-9 by gelatin zymography and Western blot assays. They also decreased nuclear translocation of nuclear factor-κB (NF-κB) P50 and P65. In addition, the migration assay showed that curcumin and CA effectively inhibited the TNF-α-induced migration of HASMCs as compared with the control group. These results suggest that curcumin and CA have inhibitory effect on proanthersclerotic mechanism *in vitro*.
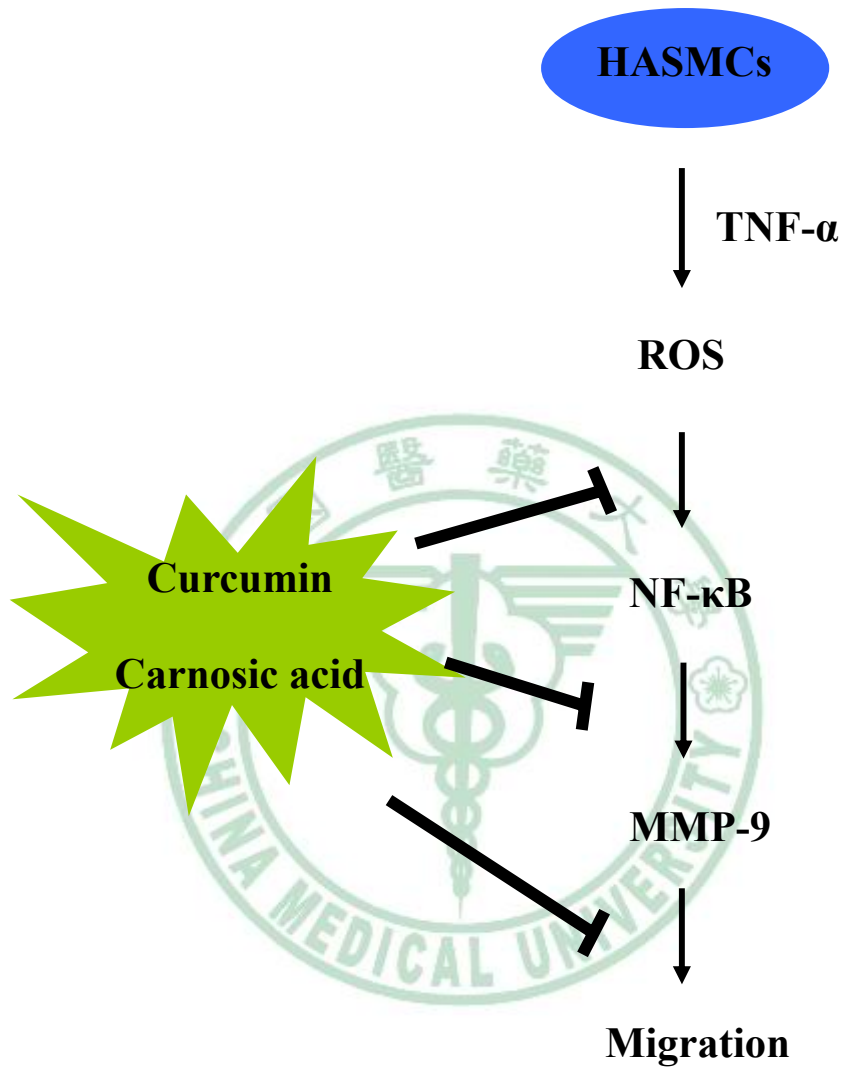
Fig. 4-1. The inhibitory effect of curcumin and carnosic acid on proanthersclerotic mechanism *in vitro*.

Reference

Aggarwal BB, Kumar A, and Bharti AC. Anticancer potential of curcumin: preclinical and clinical studies. *Anticancer Res* 23**:** 363-98, 2003.

Aggarwal BB, Shishodia S, Takada Y, Banerjee S, Newman RA, Bueso-Ramos CE, and Price JE. Curcumin suppresses the Paclitaxel-induced nuclear factor-κB pathway in breast cancer cells and inhibits lung metastasis of human breast cancer in nude mice. *Clin Cancer Res* 11: 7490-98, 2005

Aggarwal BB and Shishodia S. Molecular targets of dietary agents for prevention and therapy of cancer. *Biochem Pharmacol* 71: 1397-421, 2006.

Ahsan H, Parveen N, Khan NU, and Hadi SM. Pro-oxidant, anti-oxidant and cleavage activities on DNA of curcumin and its derivatives demethoxycurcumin and bisdemethoxycurcumin. *Chem Biol Interact* 121: 161-75, 1999.

Aruoma OI, Halliwell B, Aeschbach R, and Loliger J. Antioxidant and pro-oxidant properties of active rosemary constituents: carnosol and carnosic acid. *Xenobiotica* 22: 257-68, 1992.

Baeuerle PA. The inducible transcription activator NFκB: regulation by distinct protein subunits. *Biochim Biophys Acta* 1072: 63-80, 1991.

Baeuerle PA and Henkel T. Function and activation of NFκB in the immune system. *Annu Rev Immunol* 12: 141-79, 1994.

Baeuerle PA and Baltimore D. IκB: a specific inhibitor of the NFκB transcription factor. *Science* 242: 540-6, 1988.

Bedoui J, Oak MH, Anglard P, and Schini-Kerth VB. Catechins prevent vascular

smooth muscle cell invasion by inhibiting MT1-MMP activity and MMP-2 expression. *Cardiovasc Res* 67: 317-25, 2005.

Birkedal-Hansen H, Moore W, Bodden MK, Windsor LJ, Birkedal-Hansen B, DeCarlo A, and Engler JA. Matrix metalloproteinases: a review. *Crit Rev Oral Biol Med* 4: 197-250, 1993.

Bond M, Chase AJ, Baker AH, and Newby AC. Inhibition of transcription factor NF-κB reduces matrix metalloproteinase-1, -3 and -9 production by vascular smooth muscle cells. *Cardio Res* 50: 556-65, 2001.

Braunwald E. Shattuck lecture-cardiovascular medicine at the turn of the millennium: triumphs, concerns, and opportunities. *N Engl J Med* 337: 1360-9, 1997.

Cheng AL, Hsu CH, Lin JK, Hsu MM, Ho YF, Shen TS, Ko JY, Lin JT, Lin BR, Ming-Shiang W, Yu HS, Jee SH, Chen GS, Chen TM, Chen CA, Lai MK, Pu YS, Pan MH, Wang YJ, Tsai CC, and Hsieh CY. Phase I clinical trial of curcumin, a chemopreventive agent, in patients with high-risk or pre-malignant lesions. *Anticancer Res* 21: 2895-900, 2001.

Cho A, Graves J, and Reidy MA. Mitogen-activated protein kinases mediate matrix metalloproteinase-9 expression in vascular smooth muscle cells. *Arterioscler Thromb Vasc Biol* 20: 2527-32, 2000.

Cho A and Reidy MA. Matrix metalloproteinase-9 is necessary for the regulation of smooth muscle cell replication and migration after arterial injury. *Circ Res* 91: 845-51, 2002.

Creemers EEJM, Cleutjens JPM, Smits JFM, and Daemen MJAP. Matrix metalloproteinase inhibition after myocardial infarction: a new approach to prevent heart failure. *Circ Res* 89: 201-10, 2001.

Del-Bano MJ, Lorente J, Castillo J, Benavente-Garcia O, del Rio JA, Ortunto A, Quirin KW, and Gerard D. Phenolic diterpenes, flavones, and rosmarinic acid distribution during the development of leaves, flowers, stems, and roots of *Rosmarinus officinalis*. *J Agric Food Chem* 51: 4247-53, 2003.

Dollery CM, McEwan JR, and Henney AM. Matrix metalloproteinases and cardiovascular disease. *Circ Res* 77: 863-72, 1995.

Dschietzig T, Richter C, Pfannenschmidt G, Bartsch C, Laule M, Baumann G, and Stangl K. Dexamethasone inhibits stimulation of pulmonary endothelins by proinflammatory cytokines: possible involvement of a nuclear factor κB dependent mechanism. *Intensive Care Med* 27: 751-6, 2001.

Dzau VJ, Braun-Dullaeus R, and Sedding DG. Vascular proliferation and atherosclerosis: New perspectives and therapeutic strategies. *Nat Med* 8: 1249-56, 2002.

Fabunmi RP, Baker AH, Murray EJ, Booth RG, and Newby AC. Divergent regulation by growth factors and cytokines of 95 kDa and 72 kDa gelatinases and tissue inhibitors of metalloproteinases-1, -2 and -3 in rabbit aortic smooth muscle cells. *Biochem J* 315: 335-42, 1996.

Falk E. Pathogenesis of atherosclerosis. *Am Heart J* 138: 421-25, 1999.

Fang J, Lu J, and Holmgren A. Thioredoxin reductase is irreversibly modified by curcumin: a novel molecular mechanism for its anticancer activity. *J Biol Chem* 280: 25284-90, 2005.

Fini ME, Bartlett JD, and Matsubara M. The rabbit gene for 92-kDa matrix metalloproteinase: Role of AP1 and AP2 in cell type-specific transcription. *J Biol Chem* 269: 28620-8.

Galis ZS, Muszynski M, Sukhova GK, Simon-Morrissey E, Unemori EN, Lark MW, Amento E, and Libby P. Cytokine stimulated human vascular smooth muscle cells synthesize a complement of enzymes required for extracellular matrix digestion. *Circ Res* 75: 181-89, 1994.

Galis ZS, Johnson C, Godin D, Magid R, Shipley JM, Senior RM, and Ivan E. Targeted disruption of the matrix metalloproteinase-9 gene impairs smooth muscle cell migration and geometrical arterial remodeling. *Circ Res* 91: 852-59, 2002.

Gafner S, Lee SK, and Guendet M. Biologic evaluation of curcumin and structural derivatives in cancer chemoprevention model systems. *Phytochemistry* 65: 2849-59, 2004.

Geleijnse JM, Launer LJ, Van der Kuip DA, Hofman A, and Witteman JC. Inverse association of tea and flavonoid intakes with incident myocardial infarction: the Rotterdam Study. *Am J Clin Nutr* 75: 880-86, 2002.

Ghosh, S, May MJ, and Kopp EB. NF-kappaB and Rel proteins: evolutionary conserved mediators of immune responses. *Annu Rev Immunol* 16: 225-60, 1998.

Griendling KK, Ushio-Fukai M, Lassegue B, and Alexander RW. Angiotensin II signaling in vascular smooth muscle: new concepts. *Hypertension* 29: 366-73, 1997.

Hao H, Gabbiani G, and Bochaton-Piallat ML. Arterial smooth muscle cell heterogeneity. *Arterioscler Thromb Vasc Biol* 23: 1510-20, 2003**.**

Haraguchi H, Saito T, Okamura N, and Yagi A. Inhibition of lipid peroxidation and superoxide generation by diterpenoids from *Rosmarinus officinalis. Planta Med* 61: 333-36, 1995.

Heath DD, Pruitt MA, Brenner DE, and Rock CL. Curcumin in plasma and urine: quantitation by high-performance liquid chromatography. *J Chromatogr B* 783:

287-95, 2003.

Huang MT, Ho CT, Wang ZY, Ferraro T, Lou YR, and Stauber K. Inhibition of skin tumorigenesis by rosemary and its constituents carnosol and ursolic acid. *Cancer Res* 54: 701-8, 1994.

Huang SC, Ho CT, Lin-Shiau SY, and Lin JK. Carnosol inhibits the invasion of B16/F10 mouse melanoma cells by suppressing metalloproteinase-9 through down-regulating nuclear factor-kappaB and c-Jun. *Biochem Pharmacol* 69: 221-32, 2005.

Huang SS and Zheng RL. Rosmarinic acid inhibits angiogenesis and its mechanism of action in vitro. *Cancer Lett* 219: 1-10, 2005.

Jackson LA, Campbell LA, Schmidt RA, Kuo CC, Cappuccio AL, and Lee MJ. Specificity of detection of *Chlamydia pneumoniae* in cardiovascular atheroma: evaluation of the innocent bystander hypothesis. *Am J Pathol* 150: 1785-90, 1997.

Jones CB, Sane DC, and Herrington DM. Matrix metalloproteinases: A review of their structure and role in acute coronary syndrome. *Cardio Res* 59: 812-23, 2003.

Kaperonis EA, Liapis CD, Kakisis JD, Dimitroulis D, and Papavassiliou VG. Inflammation and atherosclerosis. *Eur J Vasc Endovasc Surg* 31: 386-93, 2006.

Khoo JC, Miller E, McLoughlin P, and Steinberg D. Enhanced macrophage uptake of low density lipoprotein after self-aggregation. *Arteriosclerosis* 8: 348-58, 1988.

Kim CH and Moon SK. Epigallocatechin-3-gallate causes the p21/WAF1-mediated G1-phase arrest of cell cycle and inhibits matrix metalloproteinase-9 expression in TNF-α-induced vascular smooth muscle cells. *Arch Biochem Biophys* 435: 264-72, 2005.

Kim YM, Kim KE, Koh GY, Ho YS, and Lee KJ. Hydrogen peroxide produced by

Angiopoietin-1 mediates angiogenesis. *Cancer Res* 66: 6167-74, 2006.

Kris-Etherton PM and Keen CL. Evidence that the antioxidant flavonoids in tea and cocoa are beneficial for cardiovascular health. *Curr Opin Lipidol* 13: 41-9, 2002.

Kutuk O and Basaga H. Inflammation meets oxidation: NF-κB as a mediator of initial lesion development in atherosclerosis. *Trends Mol Med* 9: 549-57, 2003.

Lau CW, Dhillon B, Yan H, Szmiko PE, and Verma S. Adipokines: molecular links between obesity and atherosclerosis. *Am J Physiol Heart Circ Physiol* 288: 2031-41, 2005.

Lee KW, Kim JH, Lee HJ, and Surh YJ. Curcumin inhibits Phorbol Ester-induced up-regulation of cyclooxygenase-2 and MMP-9 by blocking ERK1/2 phosphorylation and NF-κB transcriptional activity in MCF10A human breast epithelial cells. *Antioxid Redox Signal* 7: 1612-20, 2005.

Leeuwen RTJ. Extracellular proteolysis and the migrating vascular smooth muscle cell. *Fibrinolysis* 10: 59-74, 1996.

Li HY, Li Y, Yan CH, Li LN, and Chen XG. Inhibition of tumour growth by S-3-1 a synthetic intermediate of Salvionolic acid A. *J Asian Nat Prod Res* 4: 271-80, 2002.

Libby P. Molecular bases of the acute coronary syndromes. *Circulation* 91: 2844-50, 1995.

Libby P. Changing concepts of atherogenesis. *J Intern Med* 247: 349-58, 2000.

Libby P. Inflammation in atherosclerosis. *Nature* 420: 868-74, 2002.

Lo AH, Liang YC, Lin-Shiau SY, Ho CT, and Lin JK. Carnosol, an antioxidant in rosemary, suppresses inducible nitric oxide synthase through down-regulating nuclear factor-κB in mouse macrophages. *Carcinogenesis* 23: 983-91, 2002.

Lowe B, Avila HA, Bloom FR, Gleeson M, and Kusser W. Quantitation of gene

expression in neural precursors by reverse-transcription polymerase chain reaction using self-quenched, fluorogenic primers. *Anal Biochem* 315: 95-105, 2003.

Lusis AJ, Fogelman AM, and Fonarow G. Genetic basis of atherosclerosis: new genes and pathways. *Circulation* 110: 1868-73, 2004.

MacSweenety STR. Pathogenesis of abdominal aortic aneurysm. *Br J Surg* 81: 935-41, 1994.

Maeda K, Kuzuya M, Cheng XW, Asai T, Kanda S, Tamaya-mori N, Sasaki T, Shibata T, and Iguchi A. Green tea catechins inhibit the cultured smooth muscle cell invasion through the basement barrier. *Atherosclerosis* 166: 23-30, 2003.

Maheshwari RK, Singh AK, Gaddipati J, and Srimal RC. Multiple biological activities of curcumin: a short review. *Life Sci* 78: 2081-7, 2006.

Majors A, Ehrhart LA, and Pezacka EH. Homocysteine as a risk factor for vascular disease: enhanced collagen production and accumulation by smooth muscle cells. *Arterioscler Thromb Vasc Biol* 17: 2074-81, 1997.

Martin R, Hoeth M, Hofer-Warbinek R, and Schmid JA. The transcription factor NF-κB and the regulation of vascular cell function. *Arterioscler Thromb Vasc Biol* 20: 83-8, 2000.

Masuda T, Inaba Y, and Takeda Y. Antioxidant mechanism of carnosic acid: structural identification of two oxidation products. *J Agric Food Chem* 49: 5560-5, 2001.

Masuda T, Inaba Y, Maekawa T, Takeda Y, Tamura H, and Yamaguchi H. Recovery mechanism of the antioxidant activity from carnosic acid quinone, an oxidized sage and rosemary antioxidant. *J Agric Food Chem* 50: 5863-9, 2002.

Mazumder A, Raghavan K, Weinstein J, Kohn KW, and Pommier Y. Inhibition of human immunodeficiency virus type-1 integrase by curcumin. *J Biochem*

Pharmacol 49: 1165-70, 1995.

Moon SK, Cho GO, Jung SY, Gal SW, Kwon TK, and Lee YC. Quercetin exerts multiple inhibitory effects on vascular smooth muscle cells: role of ERK1/2, cellcycle regulation, and matrix metalloproteinase-9. *Biochem Biophys Res Commun* 301: 1069-78, 2003.

Moon SK, Cha BY, and Kim CH. In vitro cellular aging is associated with enhanced proliferative capacity, G1 cell cycle modulation, and matrix metalloproteinase-9 regulation in mouse aortic smooth muscle cells. *Arch Biochem Biophys* 418: 39-48, 2003.

Moon SK, Cha BY, and Kim CH. ERK1/2 mediates TNF-α induced matrix metalloproteinase-9 expression in human vascular smooth muscle cells via the regulation of NF-κB and AP-1: involvement of the Ras dependent pathway. *J Cell Physiol* 198: 417-27, 2004.

Moreno S, Scheyer T, Romano CS, and Vpjnov AA. Antioxidant and antimicrobial activities of rosemary extracts linked to their polyphenol composition. *Free Radic Res* 40: 223-31, 2006.

Muller JM, Rupec RA, and Baeuerle PA. Study of gene regulation by NF-kappa B and AP-1 in response to reactive oxygen intermediates. *Methods* 11:301-12, 1997.

Nanji AA, Jokelainen K, Tipoe GL, Rahemtulla A, Thomas P, and Dannenberg AJ. Curcumin prevents alcohol-induced liver disease in rats by inhibiting the expression of NF-kappaB-dependent genes. *Am J Physiol Gastrointest Liver Physiol* 284: 321-7, 2003.

Newby AC and Zaltsman AB. Molecular mechanisms in intimal hyperplasia. *J Pathol* 190: 300-9, 2000.

Ninomiya K, Matsuda H, Shimoda H, Nishida N, Kasajima N, Yoshino T, Morikawa T, and Yoshikawa M. Carnosic acid, a new class of lipid absorption inhibitor from sage. *Bioorg Med Chem Lett* 14: 1943-6, 2004.

Nordskog BK, Blixt AD, Morgan WT, Fields WR, and Hellmann GM. Matrix-degrading and pro-inflammatory changes in human vascular endothelial cells exposed to cigarette smoke condensate. *Cardiovasc Toxicol* 3: 101-7, 2003.

Ohtani H. Stromal reaction in cancer tissue: pathophysiologic significance of the expression of matrix-degrading enzymes in relation to matrix turnover and immune/inflammatory reactions. *Pathol Int* 48: 1-9, 1998.

Oluwatuyi M, Kaatz GW, and Gibbson S. Antibacterial and resistance modifying activity of *Rosmarinus officinalis*. *Phytochemistry* 65: 3249-54, 2004.

Pearson DA, Frankel EN, Aeschbach R, and German JB. Inhibition of endothelial cell-mediated oxidation of low-density lipoprotein by rosemary and plant phenolics. *J Agric Food Chem* 45: 578-82, 1997.

Perry NS, Bollen C, Perry EK, and Ballard C. *Salvia* for dementia therapy: review of pharmacological activity and pilot tolerability clinical trial. *Biomed Pharmacother* 75: 651-9, 2003.

Rahman A, Kefer J, Bando M, Niles WD, and Malik AB. E-selectin expression in human endothelial cells by TNF-alpha-induced oxidant generation and NF-kappaB activation. *Am J Physiol* 275: 533-44, 1998.

Richheimer SL, Bailey DT, Bernart MW, Kent M, Vininski JV, and Anderson LD. Antioxidant activity and oxidative degradation of phenolic compounds isolated from rosemary. *Recent Res Dev Oil Chem* 3: 45-58, 1999.

Ross R. The pathogenesis of atherosclerosis: a perspective for the 1990s. *Nature* 362:

801-9, 1993.

Ruby AJ, Kuttan G, Babu KD, Rajasekharan KN, and Kuttan R. Anti-tumour and antioxidant activity of natural curcuminoids. *Cancer Lett* 94: 79-83, 1995.

Sato H and Seiki M. Regulatory mechanism of 92-kDa Type-IV collagenase gene expression which is associated with invasiveness of tumor cells. *Oncogene* 8: 395-405, 1993.

Shahidi F, Janitha PK, and Wanasundara PD. Phenolic antioxidants. *Crit Rev Food Sci Nutr* 32: 67-103, 1992.

Sharma RA, Gescher AJ, and Steward WP. Curcumin: the story so far. *Eur J Cancer* 41: 1955-68, 2005.

Sharma RA, McLelland HR, Hill KA, Ireson CR, Euden SA, Manson MM, Pirmohamed M, Marnett LJ, Gescher AJ, and Steward WP. Pharmacodynamic and Pharmacokinetic Study of Oral *Curcuma* Extract in Patients with Colorectal Cancer. *Clin Cancer Res* 7: 1894-900, 2001.

Shishodia S, Potdar P, Gairola CG, and Aggarwal BB. Curcumin (diferuloylmethane) down-regulates cigarette smoke-induced NF-κB activation through inhibition of IκBα kinase in human lung epithelial cells: correlation with suppression of COX-2, MMP-9 and cyclin D1. *Carcinogenesis* 24: 1269-79, 2003.

Singh S and Aggarwal BB. Activation of transcription factor NF-κB is suppressed by Curcumin (Diferulolylmethane). *J Biol Chem* 270: 24995-50, 1995.

Somasundaram S, Edmund NA, Moore DT, Small GW, Shi YY, and Orlowski RZ. Dietary curcumin inhibits chemotherapy-induced apoptosis in models of human breast cancer. *Cancer Res* 62: 3868-75, 2002.

Stringa E, Knäuper V, Murphy G, and Gavrilovic J. Collagen degradation and

platelet-derived growth factor stimulate the migration of vascular smooth muscle cells. *J Cell Sci* 113: 2055-64, 2000.

Surh YJ. Anti-tumor promoting potential of selected spice ingredients with antioxidative and anti-inflammatory activities: a short review. *Food Chem Toxicol* 40: 1091-97, 2002.

Swarnakar S, Ganguly K, Kundu P, Banerjee A, Maity P, and Sharma AV. Curcumin regulates expression and activity of Matrix Metalloproteinases 9 and 2 during prevention and healing of Indomethacin-induced gastric ulcer. *J Biol Chem* 280: 9409-15, 2005.

Schmidt AM, Yan SD, Wautier JL, Wautier JL, and Stern D. Activation of receptor for advanced glycation end products: a mechanism for chronic vascular dysfunction in diabetic vasculopathy and atherosclerosis. *Circ Res* 84: 489-97, 1999.

Shishodia S, Sethi G, and Aggarwal BB. Curcumin: getting back to the roots. *Ann N Y Acad Sci* 1056: 206-17, 2005.

Taniyama Y and Griendling KK. Reactive oxygen species in the vasculature. *Hypertension* 42: 1075-81, 2003.

Ulubelen A, Oksuz S, Topcu G, Goren AC, and Voelter W. Antibacterial diterpenes from the roots of *Salvia blepharochlaena*. *J Nat Prod* 64: 549-51, 2001.

Wassmann S, Wassmann K, and Nickenig G. Modulation of oxidant and antioxidant enzyme expression and function in vascular cells. *Hypertension* 44: 381-6, 2004.

Weber AJ and De Bandt M. Angiogenesis: general mechanisms and implications for rheumatoid arthritis. *Joint Bone Spine* 67: 366-83, 2000.

Wenkert E, Fuchs A, and Mc Chesney JD. Chemical artifacts of the family Labiatae. *J Org Chem* 30: 2931-4, 1965.

Yang X, Thomas DP, Zhang X, Culver BW, Alexander BM, Murdoch WJ, Rao MNA, Tulis DA, Ren J, and Sreejayan N. Curcumin inhibits platelet-derived growth factor-stimulated vascular smooth muscle cell function and injury-induced neointima formation. *Arterioscler Thromb Vasc Biol* 26: 85-90, 2006.

Yokoo T and Kitamura M. Dual regulation of IL-1B-mediated matrix metalloproteinase-9 expression in mesangial cells by NF-kB and AP-1. *Am J Physiol* 270: 123-30, 1996.

Yu YM, Wang ZH, Liu CH, and Chen CS. Ellagic acid inhibits IL-1β-induced cell adhesion molecule expression in human umbilical vein endothelial cells. *Br J Nutr* 97: 692-8, 2007.

Yudkin JS, Stehouwer CD, Emeis JJ, and Coppack SW. C-reactive protein in healthy subjects: associations with obesity, insulin resistance, and endothelial dysfunction: a potential role for cytokines originating from adipose tissue. *Arterioscler Thromb Vasc Biol* 19: 972-8, 1999.

Zhu Y, Liao HL, Lin JHC, Verna L, and Stemerman MB. Low-density lipoprotein augments interleukin-1-induced vascular adhesion molecule expression in human endothelial cells. *Atherosclerosis* 144: 357-65, 1999.

Appendix 1

Table 1. Antioxidative capacities of curcumin *in vitro*.

	Inhibition of LDL Oxidation (IC$_{50}$, μmol/l)	DPPH radicals scavenging ability (IC$_{50}$, μmol/l)	Trolox Equivalent Antioxidant Capacity (TEAC) assay
Curcumin	2.56±0.12	45.8±0.1	2.88±0.04

All values are mean±SD. IC$_{50}$ values were obtained from the concentration response curves; n =3.